

Theory of interlayer exchange coupling

P. Bruno

Max-Planck-Institut für Mikrostrukturphysik

Weinberg 2, D-06120 Halle, germany

(November 2, 2018)

Abstract

This paper contains the notes of lectures on the theory of interlayer exchange coupling presented at the 30-th Ferienschule of the Institut für Festkörperforschung, Forschungszentrum Jülich, March 1999.

Published in “Magnetische Schichtsysteme”, edited by P.H. Dederichs and P. Grünberg (Forschungszentrum Jülich, 1999).

I. INTRODUCTION

Since its the discovery of interlayer exchange coupling [1], this phenomenon has stimulated a number theoretical investigations. Various approaches have used. These are:

- the Ruderman-Kittel-Kasuya-Yosida (RKKY) model [2–6];
- the free-electron model [7–9];
- the hole confinement model [10,11];
- the Anderson (or *sd*-mixing) model [12–14];
- *ab initio* calculations [15–30].

The mechanism which now widely accepted for the IEC is based upon quantum interferences in the spacer layer due to spin-dependent confinement [10,31–33].

These lecture notes are organized as follows. In, Section I, the quantum interferences due to confinement are discussed, and it is shown how this yields an oscillatory interlayer exchange coupling. In Section II, the theoretical basis of the one-electron approach of Section I is presented. Finally, in Section III, the effect of substitutional disorder is addressed.

II. PHYSICAL MECHANISM OF INTERLAYER EXCHANGE COUPLING IN TERMS OF QUANTUM INTERFERENCES: A HEURISTIC APPROACH

The purpose of this section is to present as simply as possible the mechanism of interlayer exchange coupling in terms of quantum interferences due to electron confinement in the spacer layer. The emphasis here will be on physical concepts rather than on mathematical rigor. This discussion is based on the one given in Ref. [32].

A. Elementary discussion of quantum confinement

For the sake of clarity, we shall first consider an extremely simplified model, namely the one-dimensional quantum well, which nevertheless contains the essential physics involved in the problem. Then, we shall progressively refine the model in order to make it more realistic.

The model consists in a one-dimensional quantum well representing the spacer layer (of potential $V = 0$ and width D), sandwiched between two “barriers” A and B of respective widths L_A and L_B , and respective potentials V_A and V_B . Note that we use the term “barrier” in a general sense, i.e., V_A and V_B are not necessarily positive. Furthermore, the barrier widths, L_A and L_B , can be infinite.

Change of the density of states due to quantum interferences

Let us consider an electron of wavevector k^+ (with $k^+ > 0$) propagating to the right in the spacer layer; as this electrons arrives on barrier B , it is partially reflected to the left, with a (complex) anplitude $r_B \equiv |r_B|e^{i\phi_B}$. The reflected wave of wavevector k^- is in turn reflected on barrier A with an amplitude $r_A \equiv |r_A|e^{i\phi_A}$, an so on.¹ The module $|r_{A(B)}|$ of the reflection coefficient expresses the magnitude of the reflected wave, whereas the argument $\phi_{A(B)}$ represents the phase shift due to the reflection (note that the latter is not absolutely determined and depends on the choice of the coodinate origin).

The interferences between the waves due to the multiple reflections on the barriers induce a modification of the density of states in the spacer layer, for the electronic state under consideration. The phase shift resulting from a complete round trip in the spacer is

$$\Delta\phi = qD + \phi_A + \phi_B , \quad (1)$$

with

$$q \equiv k^+ - k^- . \quad (2)$$

If the interferences are constructive, i.e., if

$$\Delta\phi = 2n\pi \quad (3)$$

with n an integer, one has an increase of the density of states; conversely, if the interferences are destructive, i.e., if

$$\Delta\phi = (2n + 1)\pi \quad (4)$$

one has a reduction of the density of states. Thus, in a first approximation, we expect the modification of the density of states in the spacer, $\Delta n(\varepsilon)$, to vary with D like

$$\cos(qD + \phi_A + \phi_B) . \quad (5)$$

Furthermore, we expect that this effect will proportional to the amplitude of the reflections on barriers A and B , i.e., to $|r_A r_B|$; finally, $\Delta n(\varepsilon)$ must be proportional to the width D of the spacer and to the density of states per unit energy and unit width,

$$\frac{2}{\pi} \frac{dq}{d\varepsilon} \quad (6)$$

¹ Of course, for the one-dimensional model, one has $k^- = -k^+$; however, this property will generally not hold for three-dimensional systems to be studied below.

which includes a factor of 2 for spin degeneracy. We can also include the effect of higher order interferences due to n round trips in the spacer; the phase shift $\Delta\phi$ is then multiplied by n and $|r_A r_B|$ is replaced by $|r_A r_B|^n$. Gathering all the terms, we get,

$$\begin{aligned}\Delta n(\varepsilon) &\approx \frac{2D}{\pi} \frac{dq}{d\varepsilon} \sum_{n=1}^{\infty} |r_A r_B|^n \cos n(qD + \phi_A + \phi_B) \\ &= \frac{2}{\pi} \operatorname{Im} \left(iD \frac{dq}{d\varepsilon} \sum_{n=1}^{\infty} (r_A r_B)^n e^{niqD} \right) \\ &= \frac{2}{\pi} \operatorname{Im} \left(i \frac{dq}{d\varepsilon} \frac{r_A r_B e^{iqD}}{1 - r_A r_B e^{iqD}} \right)\end{aligned}\quad (7)$$

As will appear clearly below, it is more convenient to consider the integrated density of states

$$N(\varepsilon) \equiv \int_{-\infty}^{\varepsilon} n(\varepsilon') d\varepsilon'. \quad (8)$$

The modification $\Delta N(\varepsilon)$ of the integrated density of states due to electron confinement is

$$\begin{aligned}\Delta N(\varepsilon) &= \frac{2}{\pi} \operatorname{Im} \sum_{n=1}^{\infty} \frac{(r_A r_B)^n}{n} e^{niqD} \\ &= -\frac{2}{\pi} \operatorname{Im} \ln \left(1 - r_A r_B e^{iqD} \right)\end{aligned}\quad (9)$$

A simple graphical interpretation of the above expression can be obtained by noting that $\operatorname{Im} \ln(z) = \operatorname{Arg}(z)$, for z complex; thus, $\Delta N(\varepsilon)$ is given by the argument, in complex plane, of a point located at an angle $\Delta\phi = qD + \phi_A + \phi_B$ on a circle of radius $|r_A r_B|$ centred in 1. This graphical construction is shown in 1.

The variation of $\Delta N(\varepsilon)$ as a function of D is shown in 2, for various values of the confinement strength $|r_A r_B|$. For weak confinement (a), $\Delta N(\varepsilon)$ varies with D in sinusoidal manner. As one increases the confinement strength (b), the oscillations are distorted, due to higher order interferences. Finally, for full confinement (c), $\Delta N(\varepsilon)$ exhibits some jumps that correspond to the bound states. We note however, that the period Λ of the oscillations of $\Delta N(\varepsilon)$ does not depend on the confinement strength, but only on the wavevector $q \equiv k^+ - k^-$, namely, $\Lambda = 2\pi/q$.

So far, we have implicitly restricted ourselves to positive energy states. Negative energy states (i.e., of imaginary wavevector) are forbidden in absence of the barriers A and B , because their amplitude diverges either on the right hand side or on the left hand side, so that they cannot be normalized. This matter of fact no longer holds in the presence of the barriers if V_A (or V_B or both) is negative: the negative energy states, i.e., varying exponentially in the spacer, can be connected to allowed states of A or B . In order to treat these states consistently, we simply have to extend the concept of reflection coefficient to states of imaginary wavevector, which is straightforward. One can check that, with this generalization, 9 accounts properly for the contribution of the evanescent states. Physically, this can be interpreted as a coupling of A and B by tunnel effect.

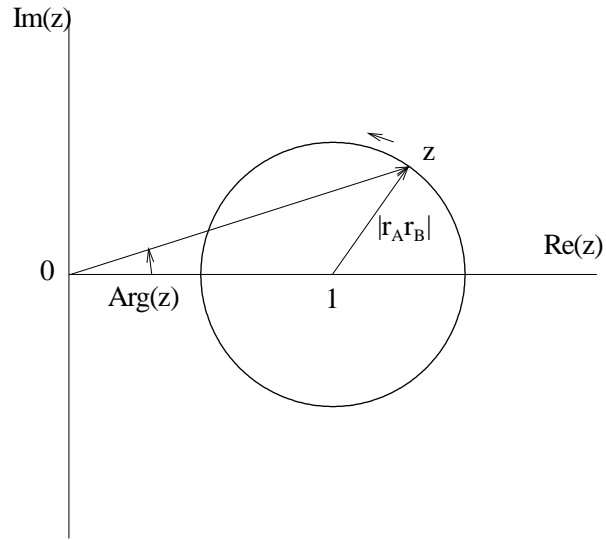


FIG. 1. Graphical interpretation of equation (9).

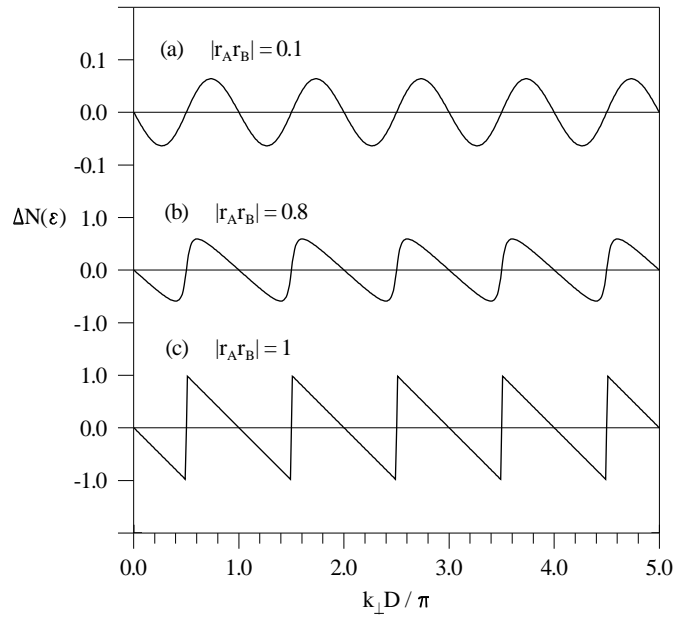


FIG. 2. Variation of $\Delta N(\varepsilon)$ as a function of D , for various values of the confinement strength: (a) $|r_A r_B| = 0.1$, (b) $|r_A r_B| = 0.8$, (c) $|r_A r_B| = 1$ (full confinement). Note the different scales along the ordinate axis.

Energy associated with the quantum interferences in the spacer

Let us now study the modification of the energy of the system due to the quantum interferences. In order to conserve the total number of electron, it is convenient to work within the grand-canonical ensemble, and to consider the thermodynamic grand-potential, which is given by

$$\begin{aligned}\Phi &\equiv -k_B T \int_{-\infty}^{+\infty} \ln \left[1 + \exp \left(\frac{\varepsilon_F - \varepsilon}{k_B T} \right) \right] n(\varepsilon) d\varepsilon \\ &= - \int_{-\infty}^{+\infty} N(\varepsilon) f(\varepsilon) d\varepsilon.\end{aligned}\quad (10)$$

At $T = 0$, this reduces to

$$\begin{aligned}\Phi &\equiv \int_{-\infty}^{\varepsilon_F} (\varepsilon - \varepsilon_F) n(\varepsilon) d\varepsilon \\ &= - \int_{-\infty}^{\varepsilon_F} N(\varepsilon) d\varepsilon.\end{aligned}\quad (11)$$

The energy ΔE associated with the interferences is the contribution to Φ corresponding to $\Delta N(\varepsilon)$,

$$\Delta E = \frac{2}{\pi} \text{Im} \int_{-\infty}^{+\infty} \ln \left(1 - r_A r_B e^{iqD} \right) d\varepsilon.\quad (12)$$

Three-dimensional layered system

The generalization of the above discussion to the more realistic case of a three-dimensional layered system is immediate. Since the system is invariant by translation parallelly to the plane, so that the in-plane wavevector \mathbf{k}_{\parallel} is a good quantum number. Thus, for a given \mathbf{k}_{\parallel} , one has an effective one-dimensional problem analogous to the one discussed above. The resulting effect of quantum interferences is obtained by summing over \mathbf{k}_{\parallel} . The modification of integrated density of states per unit area is

$$\Delta N(\varepsilon) = - \frac{1}{2\pi^3} \text{Im} \int d^2 \mathbf{k}_{\parallel} \ln \left(1 - r_A r_B e^{iq_{\perp} D} \right), \quad (13)$$

and the coupling energy per unit area is

$$\Delta E = \frac{1}{2\pi^3} \text{Im} \int d^2 \mathbf{k}_{\parallel} \int_{-\infty}^{+\infty} f(\varepsilon) \ln \left(1 - r_A r_B e^{iq_{\perp} D} \right) d\varepsilon. \quad (14)$$

Quantum size effect in an overlayer

The case of a thin overlayer deposited on a substrate is of considerable interest. In this case, one of the barriers (say, A) consists of the vacuum, and barrier B is constituted by the substrate itself. The potential of the vacuum barrier is $V_{\text{vac}} = \varepsilon_F + W$, where W is

the the work function; thus it is perfectly reflecting for occupied states, i.e., $|r_{\text{vac}} + 1|$. On the other hand, the reflection on the substrate (or coefficient r_{sub}) may be total or partial, depending on the state under consideration.

The spectral density of the occupied states in the overlayer can be investigated experimentally by photoemission spectroscopy; in addition, by using inverse photoemission, one can study the unoccupied states. If furthermore these techniques are used in the “angle-resolved” mode, they give information on the spectral density *locally in the \mathbf{k}_{\parallel} plane*.

For a given thickness of the overlayer, the photoemission spectra (either direct or inverse) exhibit some maxima and minima corresponding, respectively, to the energies for which the interferences are constructive and destructive. When the confinement is total, narrow peaks can be observed, which correspond to the quantized confined states in the overlayer, as was pointed out by Loly and Pendry [34].

Quantum size effects due to electron confinement in the photoemission spectra of overlayers have been observed in various non-magnetic systems [35–43] In particular, the systems Au(111)/Ag/vacuum and Cu(111)/Ag/vacuum offer excellent examples of this phenomenon [40,42].

Paramagnetic overlayer on a ferromagnetic substrate: Spin-polarized quantum size effect

So far our discussion concerned exclusively non-magnetic systems. Qualitatively new behavior can be expected some of the layers are ferromagnetic. case of particular interest is the one of a paramagnetic overlayer on a ferromagnetic substrate.

In the interior of the overlayer, the potential is independent of the spin; therefore the propagation of electrons is described by a wave vector k_{\perp} which is spin-independent. The reflection coefficient on the vacuum barrier, r_{vac} , is also spin-independent. However, the ferromagnetic substrate constitutes a spin-dependent potential barrier; thus, the substrate reflection coefficients for electrons with a spin parallel to the majority and minority spin directions of the substrate, respectively $r_{\text{sub}}^{\uparrow}$ and $r_{\text{sub}}^{\downarrow}$. It is convenient to define the spin average

$$\bar{r}_{\text{sub}} \equiv \frac{r_{\text{sub}}^{\uparrow} + r_{\text{sub}}^{\downarrow}}{2} \quad (15)$$

and the spin asymmetry

$$\Delta r_{\text{sub}} \equiv \frac{r_{\text{sub}}^{\uparrow} - r_{\text{sub}}^{\downarrow}}{2}. \quad (16)$$

In this case, the electron confinement in the overlayer gives rise to a spin-dependent modulation of the spectral density versus overlayer thickness; the period of the modulation is the same for both spins, whereas the amplitude and phase are expected to be spin-dependent.

The quantum size effects in paramagnetic overlayers on a ferromagnetic substrate have been investigated by several groups [44–55]. The systems studied most are Cu overlayers on a Co(001) substrate and Ag overlayers on a Fe(001) substrate. Ortega and Himpsel [45,46] observed a quantum size effect in the normal-emission photoelectron spectra of copper overlayer on fcc cobalt (001) substrate. They observed peaks due to quantum size effects both in the photoemission and in the inverse photoemission spectra an oscillation of the photoemission intensity. These quantum size effects manifest themselves also by an oscillatory behavior of the photoemission intensity at the Fermi level; as the observed oscillation period (5.9 atomic layers) is close to the long period of interlayer exchange coupling oscillations in Co/Cu(001)/Co, they pointed out that the two phenomena are related to each other; they also claimed that the observed oscillations in photoemission are spin dependent and due mostly to minority electrons. A direct confirmation of this conjecture has been given independently by Garrison *et al.* [48] and by Carbone *et al.* [49] by means of spin-polarized photoemission. They found that both the intensity and the spin-polarization exhibit an oscillatory behavior with the same period (5 – 6 atomic layers), but they have opposite phases, which indicates that the quantum size effect does indeed take place predominantly in the minority-spin band as proposed by Ortega and Himpsel [45,46]. Recently, Kläsger *et al.* [55] have observed spin-polarized quantum size effects in a copper overlayer on cobalt (001) for a non-zero in-plane wave vector corresponding to the short period oscillation of interlayer exchange coupling in Co/Cu(001)/Co; they observed short period oscillations of the photoemission intensity in good agreement with the short period oscillations of interlayer coupling. This observation provides a further confirmation of the relation between quantum size effects in photoemission and oscillation of interlayer exchange coupling.

Photoemission studies of quantum size effects have also been performed in other kinds of systems such as ferromagnetic overlayer on a non-magnetic substrate, or systems comprising more layers [56–60].

Photoemission spectroscopy undoubtedly constitutes a method of choice for investigating quantum size effects in metallic overlayers: this is due to its unique features, which allow selectivity in energy, in-plane wave vector, and spin.

Besides photoemission, spin-polarized quantum size effects in paramagnetic overlayers on a ferromagnetic substrate are also responsible for oscillatory behavior (versus overlayer thickness) of spin-polarized secondary electron emission [61,62], linear [63–68] and non-linear [69,70] magneto-optical Kerr, and magnetic anisotropy [71,72]. However, these effects usually involve a summation over all electronic states, so that the quantitative analysis of the quantum size effects may be fairly complicated.

B. Interlayer exchange coupling due to quantum interferences

Let us now consider the case of a paramagnetic layer sandwiched between two ferromagnetic barriers A and B . Now, the reflection coefficients on both sides of the paramagnetic spacer layer are spin dependent. *A priori* the angle θ between the magnetizations of the two ferromagnetic can take any value; however, for the sake of simplicity, we shall restrict ourselves here to the ferromagnetic (F) configuration (i.e., $\theta = 0$) and the antiferromagnetic (AF) one (i.e., $\theta = \pi$).

For the ferromagnetic configuration, the energy per unit area due to quantum interference is easily obtained from 14, i.e.,

$$\Delta E_F = \frac{1}{4\pi^3} \text{Im} \int d^2\mathbf{k}_{\parallel} \int_{-\infty}^{+\infty} f(\varepsilon) \left[\ln \left(1 - r_A^{\uparrow} r_B^{\uparrow} e^{iq_{\perp} D} \right) + \ln \left(1 - r_A^{\downarrow} r_B^{\downarrow} e^{iq_{\perp} D} \right) \right] d\varepsilon. \quad (17)$$

In this equation, the first and the second term correspond respectively to majority- and minority-spin electrons. The antiferromagnetic configuration is obtained by reversing the magnetization of B , i.e., by interchanging r_B^{\uparrow} and r_B^{\downarrow} ; thus the corresponding energy per unit area is

$$\Delta E_{AF} = \frac{1}{4\pi^3} \text{Im} \int d^2\mathbf{k}_{\parallel} \int_{-\infty}^{+\infty} f(\varepsilon) \left[\ln \left(1 - r_A^{\uparrow} r_B^{\downarrow} e^{iq_{\perp} D} \right) + \ln \left(1 - r_A^{\downarrow} r_B^{\uparrow} e^{iq_{\perp} D} \right) \right] d\varepsilon. \quad (18)$$

Thus, the interlayer exchange coupling energy is

$$E_F - E_{AF} = \frac{1}{4\pi^3} \text{Im} \int d^2\mathbf{k}_{\parallel} \int_{-\infty}^{+\infty} f(\varepsilon) \ln \left[\frac{\left(1 - r_A^{\uparrow} r_B^{\uparrow} e^{iq_{\perp} D} \right) \left(1 - r_A^{\downarrow} r_B^{\downarrow} e^{iq_{\perp} D} \right)}{\left(1 - r_A^{\uparrow} r_B^{\downarrow} e^{iq_{\perp} D} \right) \left(1 - r_A^{\downarrow} r_B^{\uparrow} e^{iq_{\perp} D} \right)} \right] d\varepsilon \quad (19)$$

which can be simplified as

$$E_F - E_{AF} \approx - \frac{1}{\pi^3} \text{Im} \int d^2\mathbf{k}_{\parallel} \int_{-\infty}^{\infty} f(\varepsilon) \Delta r_A \Delta r_B e^{iq_{\perp} D} d\varepsilon \quad (20)$$

in the limit of weak confinement. The above expression for the IEC has a rather transparent physical interpretation. First, as the integrations on \mathbf{k}_{\parallel} over the first two-dimensional Brillouin zone and on the energy up to the Fermi level show, the IEC is a sum of contributions from all occupied electronic states. The contribution of a given electronic state, of energy ε and in-plane wavevector \mathbf{k}_{\parallel} , consists of the product of three factors: the two factors Δr_A and Δr_B express the spin-asymmetry of the confinement due to the magnetic layers A and B , respectively, while the exponential factor $e^{iq_{\perp} D}$ describes the propagation through the spacer and is responsible for the interference (or quantum size) effect. Thus, this approach establishes an explicit and direct link between oscillatory IEC and quantum size effects such as observed in photoemission.

Asymptotic behavior for large spacer thicknesses

In the limit of large spacer thickness D , the exponential factor oscillates rapidly with ε and \mathbf{k}_{\parallel} , which leads to some cancellation of the contributions to the IEC due to the different electronic states. However, because the integration over energy is abruptly stopped

at ε_F , states located at the Fermi level give predominant contributions. Thus the integral on ε may be calculated by fixing all other factors to their value at ε_F , and by developing $q_{\perp} \equiv k_{\perp}^+ - k_{\perp}^-$ around ε_F , i.e.,

$$q_{\perp} \approx q_{\perp F} + 2 \frac{\varepsilon - \varepsilon_F}{\hbar v_{\perp F}^{+-}}, \quad (21)$$

with

$$\frac{2}{v_{\perp F}^{+-}} \equiv \frac{1}{v_{\perp F}^+} - \frac{1}{v_{\perp F}^-}. \quad (22)$$

The integration (see Ref. [32] for details) yields

$$E_F - E_{AF} = \frac{1}{2\pi^3} \text{Im} \int d^2 \mathbf{k}_{\parallel} \frac{i \hbar v_{\perp F}^{+-}}{D} \Delta r_A \Delta r_B e^{iq_{\perp F} D} \times F(2\pi k_B T D / \hbar v_{\perp F}^{+-}), \quad (23)$$

where

$$F(x) \equiv \frac{x}{\sinh x}. \quad (24)$$

In the above equations, $q_{\perp F}$ is a vector spanning the *complex Fermi surface*; the velocity $v_{\perp F}^{+-}$ is a combination of the group velocities at the extremities $k_{\perp F}^+$ and $k_{\perp F}^-$.

Next, the integration on \mathbf{k}_{\parallel} is performed by noting, that, for large spacer thickness D , the only significant contributions arise from the neighboring of critical vectors $\mathbf{k}_{\parallel}^{\alpha}$ where $q_{\perp F}$ is stationary. Around such vectors, $q_{\perp F}$ may be expanded as

$$q_{\perp F} = q_{\perp F}^{\alpha} - \frac{(k_x - k_x^{\alpha})^2}{\kappa_x^{\alpha}} - \frac{(k_y - k_y^{\alpha})^2}{\kappa_y^{\alpha}}, \quad (25)$$

where the cross terms have been canceled by a proper choice of the axes; κ_x^{α} and κ_y^{α} are combinations of the curvature radii of the Fermi surface at $(\mathbf{k}_{\parallel}^{\alpha}, k_{\perp}^{+\alpha})$ and $(\mathbf{k}_{\parallel}^{\alpha}, k_{\perp}^{-\alpha})$.

The integral is calculated by using the stationary phase approximation, [32] and one obtains

$$J_1 = \text{Im} \sum_{\alpha} \frac{\hbar v_{\perp}^{\alpha} \kappa_{\alpha}}{4\pi^2 D^2} \Delta r_A^{\alpha} \Delta r_B^{\alpha} e^{iq_{\perp}^{\alpha} D} \times F(2\pi k_B T D / \hbar v_{\perp}^{\alpha}), \quad (26)$$

where q_{\perp}^{α} , v_{\perp}^{α} , Δr_A^{α} , Δr_B^{α} correspond to the critical vector $\mathbf{k}_{\parallel}^{\alpha}$, and

$$\kappa_{\alpha} \equiv (\kappa_x^{\alpha})^{1/2} (\kappa_y^{\alpha})^{1/2}; \quad (27)$$

in the above equation, one takes the square root with an argument between 0 and π .

This analysis shows that *in fine*, the only remaining terms in the limit of large spacer thickness D arise from the neighborhood of states having in-plane wavevectors $\mathbf{k}_{\parallel}^{\alpha}$ such that the spanning vector of the Fermi surface $q_{\perp F} = k_{\perp F}^+ - k_{\perp F}^-$ is stationary with respect

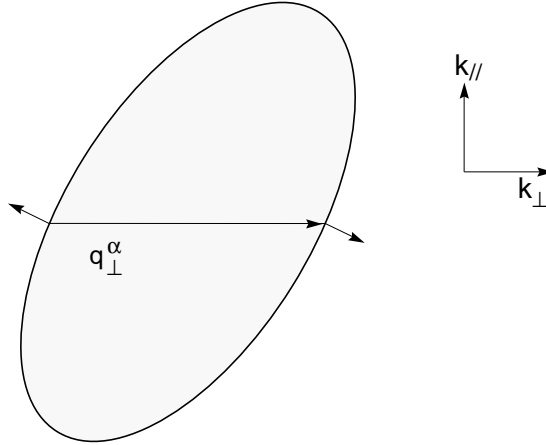


FIG. 3. Sketch showing the wavevector q_{\perp}^{α} giving the oscillation period of oscillatory inter-layer exchange coupling, for the case of a non-spherical Fermi surface.

to \mathbf{k}_{\parallel} for $\mathbf{k}_{\parallel} = \mathbf{k}_{\parallel}^{\alpha}$, and the corresponding contribution oscillates with a wavevector equal to $q_{\perp F}^{\alpha}$. This selection rule was first derived in the context of the RKKY model [4]; it is illustrated in Fig. 3. There may be several such stationary spanning vectors and, hence, several oscillatory components; they are labelled by the index α .

The above selection rule allows to predict the oscillation period(s) of the interlayer exchange coupling versus spacer thickness by just inspecting the bulk Fermi surface of the spacer material. In view of an experimental test of these predictions, noble metal spacer layers appear to be the best suited candidates; there are several reasons for this choice:

- Fermi surfaces of noble metals are known very accurately from de Haas-van Alphen and cyclotron resonance experiments [73];
- since only the sp band intersect the Fermi level, the Fermi surface is rather simple, and does not depart very much from a free-electron Fermi sphere;
- samples of very good quality with noble metals as a spacer layer could be prepared.

Fig. 4 shows a cross-section of the Fermi surface of Cu, indicating the stationary spanning vectors for the (001), (111), and (110) crystalline orientations [4]; the Fermi surfaces of Ag and Au are qualitatively similar. For the (111) orientation, a single (long) period is predicted; for the (001) orientation, both a long period and a short period are predicted; for the (110) orientation, four different periods are predicted (only one stationary spanning vector is seen in figure 4, the three others being located in other cross-sections of the Fermi surface). These theoretical predictions have been confirmed successfully by numerous experimental observations. In particular, the coexistence of a long and a short period for the (001) orientation has been confirmed for Cu [74,75], Ag

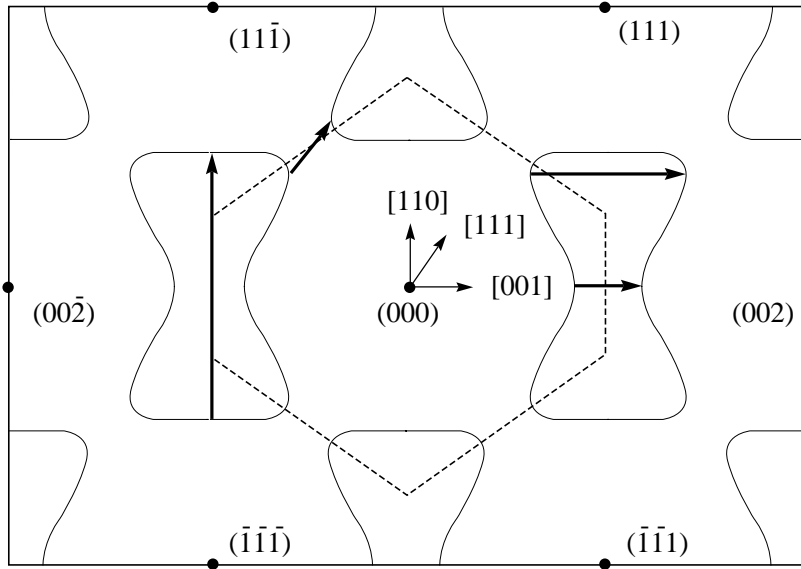


FIG. 4. Cross section of the Fermi surface of Cu along the $(1\bar{1}0)$ plane passing through the origin. The solid dots indicate the reciprocal lattice vectors. The dashed lines indicate the boundary of the first Brillouin zone. The solid arrows, respectively horizontal, oblique, and vertical, indicate the vectors q_{\perp}^{α} giving the oscillation period(s), respectively for the (001) , (111) , and (110) orientations.

[76], and Au [77–79]; and the experimental periods have been found to be in excellent agreement with the theoretical ones.

In a further attempt to test the theoretical predictions for the periods of oscillatory coupling, several groups [84–86] have undertaken to modify in a controlled manner the size of the Fermi surface (and hence, the period of the coupling) by alloying the spacer noble metal (Cu) with a metal of lower valence (Ni); in both cases, the change in oscillation period due to alloying has been found in good agreement with the expected change in the Fermi surface.

Although the asymptotic approximation is often an excellent one to describe the IEC, in cases where the reflection coefficients vary strongly with ε and \mathbf{k}_{\parallel} near the stationary spanning vectors q_{\perp}^{α} of the spacer Fermi surface, preasymptotic corrections need to be considered. A detailed discussion of the preasymptotic corrections is presented in Ref. [87].

Effect of magnetic layer thickness

As already mentioned, the influence of the IEC on the ferromagnetic layer thickness is contained in the reflection coefficients Δr_A and Δr_B . If the ferromagnetic layers are of finite thickness, reflections usually may take place at the two interfaces bounding the

TABLE I. Comparison between the theoretical predictions of Ref. [4] and experimental observations for the oscillation periods of interlayer exchange coupling versus overlayer thickness.

spacer	theoretical periods	system	experimental periods	Ref.
Cu(111)	$\Lambda = 4.5$ AL	Co/Cu/Co(111)	$\Lambda \approx 5$ AL	[80]
		Co/Cu/Co(111)	$\Lambda \approx 6$ AL	[81]
		Fe/Cu/Fe(111)	$\Lambda \approx 6$ AL	[82]
Cu(001)	$\Lambda_1 = 2.6$ AL $\Lambda_2 = 5.9$ AL	Co/Cu/Co(001)	$\Lambda \approx 6$ AL	[83]
		Co/Cu/Co(001)	$\Lambda_1 \approx 2.6$ AL	[74]
			$\Lambda_2 \approx 8$ AL	
		Co/Cu/Co(001)	$\Lambda_1 \approx 2.7$ AL	[75]
			$\Lambda_2 \approx 6.1$ AL	
Ag(001)	$\Lambda_1 = 2.4$ AL $\Lambda_2 = 5.6$ AL	Fe/Ag/Fe(001)	$\Lambda_1 \approx 2.4$ AL	[76]
			$\Lambda_2 \approx 5.6$ AL	
Au(001)	$\Lambda_1 = 2.5$ AL $\Lambda_2 = 8.6$ AL	Fe/Au/Fe(001)	$\Lambda_1 \approx 2$ AL	[77]
			$\Lambda_2 \approx 7-8$ AL	
		Fe/Au/Fe(001)	$\Lambda_1 \approx 2.5$ AL	[78,79]
			$\Lambda_2 \approx 8.6$ AL	

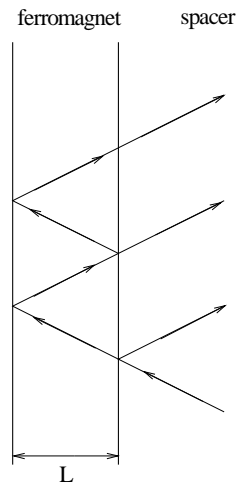


FIG. 5. Sketch of the waves contributing to the net reflection coefficient on a ferromagnetic layer of finite thickness L .

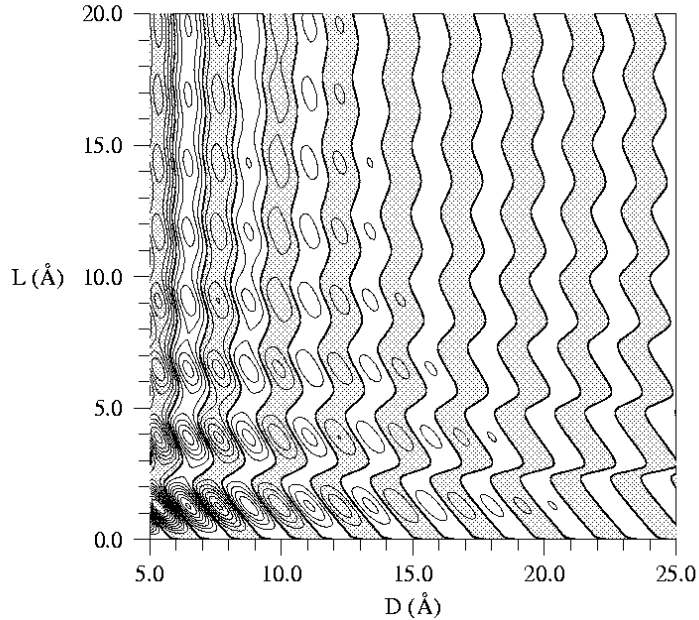


FIG. 6. Contour plot of the interlayer exchange coupling constant $J \equiv (E_F - E_{AF})/2$ vs spacer thickness D and magnetic layer thickness L , calculated within the free-electron model (see Ref. [32] for details). The spacing between successive contour lines is 40×10^{-3} erg cm $^{-2}$; the shaded area corresponds to antiferromagnetic coupling.

ferromagnetic layers, as sketched in Fig. 5, giving rise to interferences [88], and hence, to oscillations of the IEC versus ferromagnetic layers thickness. A more detailed discussion of this effect is given in Refs. [32,88]. This behavior was first predicted from calculations based upon a free-electron model [7]. On the experimental point of view, it was confirmed by Bloemen *et al.* [89] in Co/Cu/Co(001) and by Okuno and Inomata [90] in Fe/Cr/Fe(001). The amplitude of the oscillations of the IEC versus ferromagnetic layers thickness is generally much smaller than the oscillations versus spacer thickness, and do not give rise to changes of sign of the IEC. This is illustrated in Fig. 6.

Effect of overlayer thickness

A more (*a priori*) surprising behavior is the dependence of the IEC on the thickness of the protective overlayer. From a naïve point of view, one might think that layers external to the basic ferromagnet/spacer/ferromagnet sandwich should not influence the interaction between the two ferromagnetic layers. This view is incorrect, in particular when the system is covered by an ultrathin protective overlayer. In this case, the electrons

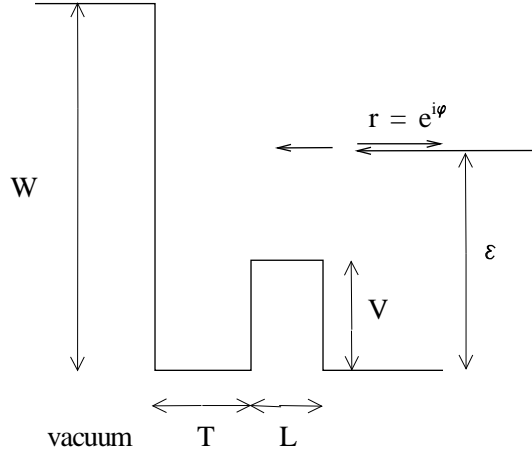


FIG. 7. Sketch of the model used to discuss the influence of the overlayer and vacuum barrier on the reflection coefficient.

are able to reach the vacuum barrier, which is a perfectly reflecting one, so that strong confinement and interference effects take place in the overlayer, which lead to a weak but sizeable oscillatory variation of the IEC as a function of the overlayer thickness.

Here, we illustrate the effect of interferences in the overlayer by means of the simple model depicted in Fig. 7. An electron of energy ε and in-plane wave vector $k_{\parallel} = 0$ is incoming from the right. The magnetic layer is represented by a barrier of height V and width L ; the overlayer has a thickness T , and the vacuum is modeled by a semi-infinite potential barrier of height W . The spin dependence of the magnetic barrier is not considered here.

Since the energy of the incoming electron is smaller than the vacuum barrier height, particle flux conservation imposes to have $|r| = 1$, and the reflection coefficient may be written as $r = e^{i\phi}$. It is thus sufficient to discuss the behavior of the reflection phase shift ϕ . The variation of ϕ as a function of the overlayer thickness T is shown in Fig. 8. The behavior is very contrasted, depending on the value of V . Two limit cases can be considered.

In the first case, V is small as compared to ε , the reflection phase shift is essentially given by the sum of the phase shift due to the reflection on vacuum and of the one due to the round trip through the magnetic layer and the overlayer, so that one has a linear variation of ϕ versus T , as appears in Fig. 8 for $V = 0$ and $V = 0.5$ eV. Thus, the reflection coefficient $r = e^{i\phi}$ varies periodically versus overlayer thickness T , with a period equal to $2\pi/q_{\perp}$. The change of phase shift as V varies is due to the change in the phase shift associated with the travel through the magnetic layer.

The opposite limit case is obtained when $\varepsilon < V$; in this case, r is essentially constant,

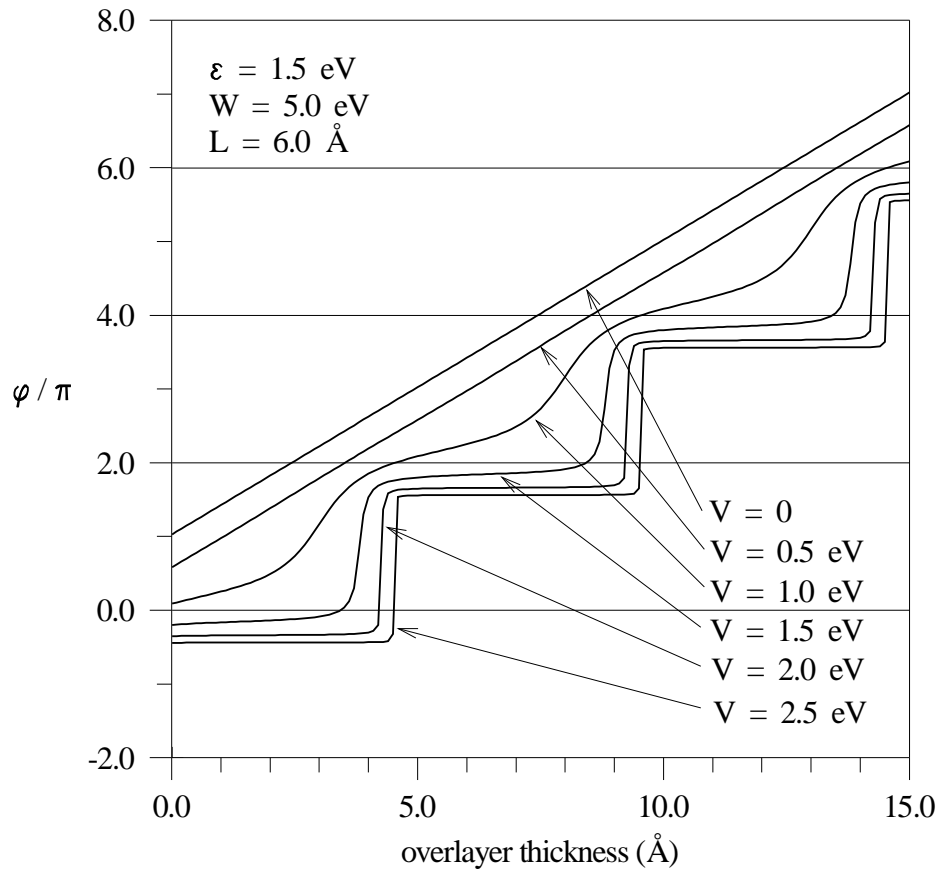


FIG. 8. Variation of the reflection phase shift ϕ versus overlayer thickness T for various values of the height V of the magnetic barrier, as indicated by the arrows. Parameters: $\varepsilon = 1.5 \text{ eV}$, $W = 5.0 \text{ eV}$, $L = 6.0 \text{ \AA}$.

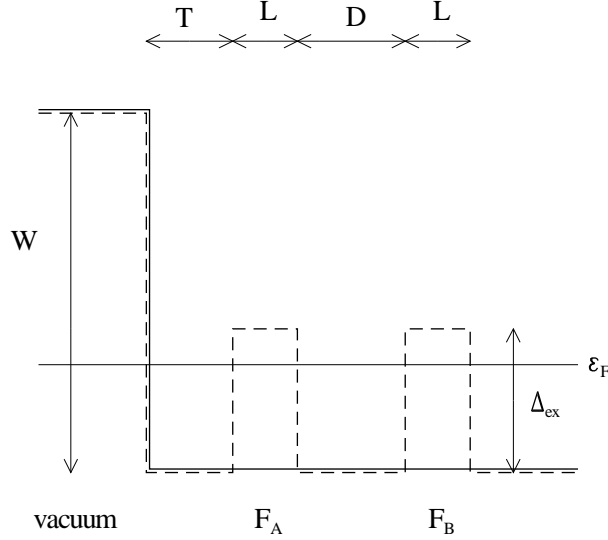


FIG. 9. Sketch of the model used to discuss the influence of the overlayer and vacuum barrier on the interlayer exchange coupling; the solid and dashed line represent, respectively, the majority spin and minority spin potential profiles, for the configuration of ferromagnetic alignment.

except for resonances where ϕ makes a jump of 2π , corresponding to the crossing quasi-bound states in the overlayer. This is clearly demonstrated in Fig. 8, for $V = 2.0$ eV and $V = 2.5$ eV. As the transmission through the magnetic barrier decreases, the resonances become narrower and their effect is completely negligible.

The intermediate situation evolves continuously between the two limit cases, as the curves corresponding to $V = 1.0$ eV and $V = 1.5$ eV in Fig. 8 show.

With help of the above argument, we can understand easily how the thickness of the overlayer influences the IEC. As will be discussed below, the variation of the interlayer coupling versus overlayer thickness T has a completely different behavior, depending on whether the magnetic barrier strongly confines the minority spin electrons at Fermi level (i.e., $\epsilon_F < \Delta_{\text{ex}}$) or not; for brevity, in the following these two opposite situations will be referred to as strong confinement and weak confinement, respectively.

Let us consider first the case of weak confinement. In this case, one finds that the IEC dependence upon overlayer thickness T is via an oscillatory function of $T + D$, as appears clearly from Fig. 10 (top).

On the other hand, for the strong confinement case, as Fig. 10 (bottom) shows, the interferences in the overlayer have only a small influence and yields a small modulation of the coupling strength as T varies.

This effect, which follows directly from the quantum interference (or quantum size effect) mechanism, has been proposed and experimentally confirmed independently by de Vries *et al.* [91] for the Co/Cu/Co(001) system with a Cu(001) overlayer, by Okuno and Inomata [92] for the Fe/Au/Fe(001) system with a Au(001) overlayer, and by Bounouh

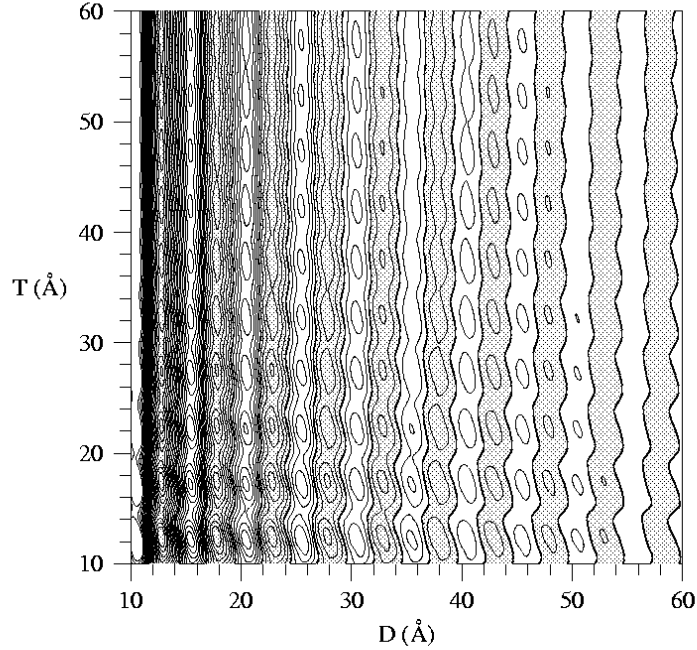
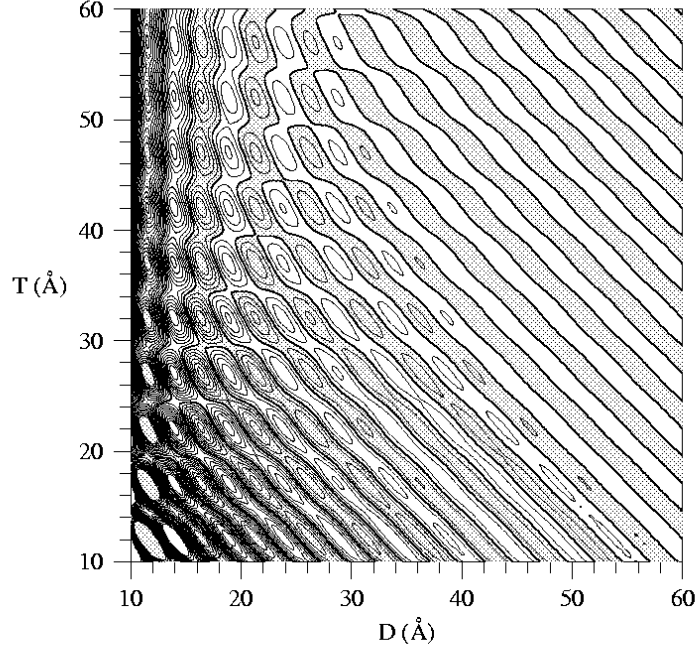


FIG. 10. Contour plot of the interlayer exchange coupling, $E_F - E_{AF}$, versus spacer thickness D and overlayer thickness T . Parameters: top pannel: $\varepsilon_F = 1.5$ eV, $W = 5.0$ eV, $\Delta_{\text{ex}} = 0.5$ eV, $L = 6.0$ Å; bottom pannel: $\varepsilon_F = 1.5$ eV, $W = 5.0$ eV, $\Delta_{\text{ex}} = 2.0$ eV, $L = 6.0$ Å. The spacing between successive contour lines is repectively 2.0×10^{-3} erg.cm $^{-2}$ and 0.2 erg.cm $^{-2}$ in the top and bottom pannels; the shaded area corresponds to antiferromagnetic coupling.

TABLE II. Comparison between the theoretical predictions of Ref. [94] and experimental observations for the oscillation periods of interlayer exchange coupling versus overlayer thickness.

overlayer	theoretical periods	system	experimental periods	Ref.
Cu(001)	$\Lambda_1 = 2.6$ AL	Cu/Co/Cu/Co/Cu(001)	$\Lambda \approx 5$ AL	[91]
	$\Lambda_2 = 5.9$ AL			
Au(001)	$\Lambda_1 = 2.5$ AL	Au/Fe/Au/Fe/Au(001)	$\Lambda_1 \approx 2.6$ AL	[92]
	$\Lambda_2 = 8.6$ AL			
Au(111)	$\Lambda = 4.8$ AL	Au/Co/Au/Co/Au(111)	$\Lambda \approx 5$ AL	[93]

et al. [93] for the Co/Au/Co(0001) with a Au(111) overlayer. In both cases, the observed period(s) for the oscillations versus overlayer thickness were found to be in good agreement with the theoretically predicted ones. This effect has also been confirmed by means of first-principles calculations for the Co/Cu/Co(001) with a Cu overlayer [95]. The comparison between the periods of oscillations versus overlayer thickness predicted theoretically and those observed experimentally is given in Table II.

III. EXCHANGE INTERACTIONS WITHIN DENSITY FUNCTIONAL THEORY

The mechanism of IEC presented above is based upon an independent electron picture. That such a picture is actually valid is not immediately obvious, in view of the fact that exchange interactions are indeed due to the Coulomb interaction between electrons. In this Section, we present the justification of the independent electron picture for the IEC. It relies on the use of “force theorems” for the magnetic interactions, which follow from variational properties of various energy functionals. Since these considerations are not particular to the problem of interlayer coupling, but apply to any kind of exchange interactions in metallic magnetic systems, a more general point of view will be adopted here.

A. Constrained density functional theory

Almost all modern methods of electronic structure calculation rely the density functional theory (DFT) of Hohenberg and Kohn [96], within the local density approximation (LDA) of Kohn and Sham [97]. In the DFT (generalized to take the spin polarization into account [98]) the system under consideration is described in terms of the local density spinor $\tilde{n}(\mathbf{r})$ whose matrix elements are given by¹

¹Throughout this paper the tilde $\tilde{}$ will be used to note spinor quantities.

$$\tilde{n}_{\alpha\beta}(\mathbf{r}) = \langle \Psi | \psi_{\alpha}^{\dagger}(\mathbf{r})\psi_{\beta}(\mathbf{r}) | \Psi \rangle. \quad (28)$$

In the above equation $\psi_{\alpha}^{\dagger}(\mathbf{r})$ ($\psi_{\beta}(\mathbf{r})$) is the second-quantization creation (destruction) operator for an electron of spin α (β) at \mathbf{r} , and $|\Psi\rangle$ is the many-body wave function. Alternatively, the system can be described in terms of the more familiar local charge and spin densities, $\rho(\mathbf{r})$ and $\mathbf{m}(\mathbf{r})$, which are related to the density spinor by

$$\rho = \text{tr}(\tilde{n}) \quad (29)$$

$$\mathbf{m} = \text{tr}(\tilde{n} \tilde{\boldsymbol{\sigma}}) \quad (30)$$

$$\tilde{n} = \frac{(\rho \tilde{\sigma}_0 + \mathbf{m} \cdot \tilde{\boldsymbol{\sigma}})}{2} \quad (31)$$

where

$$\tilde{\sigma}_0 \equiv \begin{pmatrix} 1 & 0 \\ 0 & 1 \end{pmatrix} \quad (32)$$

and

$$\tilde{\boldsymbol{\sigma}} \equiv \begin{pmatrix} \hat{\mathbf{z}} & \hat{\mathbf{x}} - i\hat{\mathbf{y}} \\ \hat{\mathbf{x}} + i\hat{\mathbf{y}} & -\hat{\mathbf{z}} \end{pmatrix} \quad (33)$$

is the vector whose components are the Pauli matrices; $\hat{\mathbf{x}}$, $\hat{\mathbf{y}}$ and $\hat{\mathbf{z}}$ are the unit vectors of the cartesian axes, and “tr” represents the trace over spin indices.

The DFT establishes that the total energy of a given system is a unique functional $\mathcal{E}[\tilde{n}]$ of the density spinor $\tilde{n}(\mathbf{r})$ which is stationary and has its absolute minimum for the density spinor $\tilde{n}_0(\mathbf{r})$ corresponding to the ground state of the system, and that the minimum energy is equal to the ground state energy, \mathcal{E}_0 , i.e.,

$$\mathcal{E}_0 = \mathcal{E}[\tilde{n}_0] = \min_{\tilde{n}} \mathcal{E}[\tilde{n}]. \quad (34)$$

The approach universally used to compute the ground state density spinor \tilde{n}_0 and the ground state energy \mathcal{E}_0 is the one proposed by Kohn and Sham [97], who rewrote the energy functional as

$$\mathcal{E}[\tilde{n}] = \mathcal{T}_0[\tilde{n}] + \mathcal{V}_{\text{ext}}[\tilde{n}] + \mathcal{U}_H[\tilde{n}] + \mathcal{E}_{\text{xc}}[\tilde{n}]. \quad (35)$$

In the above equation, the first term is the kinetic energy of a fictitious system of independent electrons having the same density spinor $\tilde{n}(\mathbf{r})$ as the real system. The second and third terms are respectively the potential energy of the electrons in the external potential and the Hartree approximation to the energy of Coulomb repulsion between electrons. The last term represents the exchange and correlation correction to the kinetic and Coulomb energies.

The Hartree and external potential terms can be calculated trivially. The exchange-correlation term cannot be calculated exactly; however, convenient and efficient approximations exist for computing it within the LDA. The most problematic term is the kinetic

energy $\mathcal{T}_0[\tilde{n}]$, for which no satisfactory approximation is known. Kohn and Sham solved the problem by showing that the system can be mapped to a fictitious system of independent electrons having the same density spinor and moving in an effective local potential spinor given by

$$\tilde{w}_{\text{eff}}[\tilde{n}](\mathbf{r}) \equiv \tilde{w}_{\text{ext}}(\mathbf{r}) + \tilde{w}_H[\tilde{n}](\mathbf{r}) + \tilde{w}_{\text{xc}}[\tilde{n}](\mathbf{r}) \quad (36)$$

where $\tilde{w}_{\text{ext}}(\mathbf{r})$ is the external potential spinor, and

$$\tilde{w}_H[\tilde{n}](\mathbf{r}) \equiv \frac{\delta \mathcal{U}_H[\tilde{n}]}{\delta \tilde{n}(\mathbf{r})} \quad (37)$$

$$\tilde{w}_{\text{xc}}[\tilde{n}](\mathbf{r}) \equiv \frac{\delta \mathcal{E}_{\text{xc}}[\tilde{n}]}{\delta \tilde{n}(\mathbf{r})} \quad (38)$$

are respectively the Hartree and exchange-correlation potential spinors. One has to solve Schrödinger-like equations for independent electrons in the effective potential spinor $\tilde{w}_{\text{eff}}[\tilde{n}]$ (Kohn-Sham equations). The ground state energy is then given by

$$\mathcal{E}_0 = \sum_{\varepsilon_i \leq \varepsilon_F} \varepsilon_i + \mathcal{V}_{\text{ext}}[\tilde{n}_0] + \mathcal{U}_H[\tilde{n}_0] + \mathcal{E}_{\text{xc}}[\tilde{n}_0] - \int d^3\mathbf{r} \text{tr}(\tilde{n}_0 \tilde{w}_{\text{eff}}[\tilde{n}_0]) \quad (39)$$

where ε_i are the single particle energies corresponding to the solutions of the Kohn-Sham equations. Since the effective potential spinor depends on the density spinor, the Kohn-Sham equations must be solved self-consistently, which is usually achieved iteratively, starting from a trial density spinor.

As it stands, this theory is not very convenient for computing exchange interactions: indeed, as it gives some information only on the ground state of a system, one would learn only which configuration of magnetic moments (e.g., ferromagnetic, antiferromagnetic, or canted) corresponds to the ground state; thus would obtain the *sign* of the interaction, but one would not learn anything about its *strength*. For this, one would have to include in the Hamiltonian the Zeeman interaction due to an external magnetic field, and compute the configuration of magnetic moments, and the total energy of the system as a function of this external field. This precisely how one proceeds in an experiment! Although this is a conceptually straightforward approach, it is not very convenient to implement, and has never been actually used.

Actually, what we would like to know is the ground state energy of the system, subjected to the restriction that the local spin-polarization $\mathbf{m}(\mathbf{r})$ is constrained to be along some prescribed direction of unit vector $\hat{\mathbf{u}}(\mathbf{r})$; the constraint may be extended to the whole space or restricted to a given subspace V . This approach relies on a particular case of the constrained density functional theory (CDFT) of Dederichs *et al* [99]. It uses the standard method of Lagrange transformation, in which one defines the new functional

$$\mathcal{F}_{\hat{\mathbf{u}}}[\tilde{n}, \mathbf{h}_{\perp \hat{\mathbf{u}}}] \equiv \mathcal{E}[\tilde{n}] - \int_V d^3\mathbf{r} \mathbf{m}(\mathbf{r}) \cdot \mathbf{h}_{\perp \hat{\mathbf{u}}}(\mathbf{r}). \quad (40)$$

The Lagrange parameter \mathbf{h}_{\perp} is a transverse magnetic field, perpendicular to the local magnetization direction $\hat{\mathbf{u}}$, to be determined self-consistently. The density spinor of the

constrained ground state $\tilde{n}_{\hat{\mathbf{u}}}^*(\mathbf{r})$, its energy $\mathcal{E}_{\text{exch}}[\hat{\mathbf{u}}]$, and the corresponding transverse field $\mathbf{h}_{\perp\hat{\mathbf{u}}}^*$ are obtained by minimizing $\mathcal{F}_{\hat{\mathbf{u}}}[\tilde{n}, \mathbf{h}_{\perp\hat{\mathbf{u}}}]$ with respect to \tilde{n} and $\mathbf{h}_{\perp\hat{\mathbf{u}}}$, i.e.,

$$\mathcal{E}[\tilde{n}_{\hat{\mathbf{u}}}^*] = \min_{\tilde{n}, \mathbf{h}_{\perp\hat{\mathbf{u}}}} \mathcal{F}_{\hat{\mathbf{u}}}[\tilde{n}, \mathbf{h}_{\perp\hat{\mathbf{u}}}] = \mathcal{F}_{\hat{\mathbf{u}}}[\tilde{n}_{\hat{\mathbf{u}}}^*, \mathbf{h}_{\perp\hat{\mathbf{u}}}^*] \quad (41)$$

$$\equiv \mathcal{E}_{\text{exch}}[\hat{\mathbf{u}}] \quad (42)$$

The physical meaning of $\mathbf{h}_{\perp\hat{\mathbf{u}}}(\mathbf{r})$ is quite clear: it is the transverse external field one needs to adjust in order to maintain everywhere the magnetization parallel to the prescribed direction $\hat{\mathbf{u}}(\mathbf{r})$. The local density of torque due to exchange interactions upon imposing the constraint $\hat{\mathbf{u}}(\mathbf{r})$ is given by

$$\mathbf{\Gamma}_{\hat{\mathbf{u}}}(\mathbf{r}) \equiv - \frac{\delta \mathcal{E}_{\text{exch}}[\hat{\mathbf{u}}]}{\delta \mathbf{\Omega}(\mathbf{r})} \quad (43)$$

where the vector $\mathbf{\Omega}(\mathbf{r})$ represents a local rotation of the spin-polarization axis. It is related to the transverse field by

$$\mathbf{\Gamma}_{\hat{\mathbf{u}}}(\mathbf{r}) = - \mathbf{m}_{\hat{\mathbf{u}}}(\mathbf{r}) \times \mathbf{h}_{\perp\hat{\mathbf{u}}}. \quad (44)$$

The constrained ground state density spinor $\tilde{n}_{\hat{\mathbf{u}}}^*$ is calculated as in the unconstrained DFT, by solving self-consistently the Kohn-Sham equations with the effective potential spinor

$$\tilde{w}_{\text{eff}}[\tilde{n}, \mathbf{h}_{\perp\hat{\mathbf{u}}}] (\mathbf{r}) = \tilde{w}_{\text{ext}}(\mathbf{r}) + \tilde{w}_H[\tilde{n}](\mathbf{r}) + \tilde{w}_{\text{xc}}[\tilde{n}](\mathbf{r}) - \mathbf{h}_{\perp\hat{\mathbf{u}}}(\mathbf{r}) \cdot \tilde{\sigma}. \quad (45)$$

The constrained ground state energy is then calculated as

$$\begin{aligned} \mathcal{E}_{\text{exch}}[\hat{\mathbf{u}}] &= \sum_{\varepsilon_i \leq \varepsilon_F} \varepsilon_i - \int d^3\mathbf{r} \text{tr} (\tilde{n}_{\hat{\mathbf{u}}}^* \tilde{w}_{\text{eff}}[\tilde{n}_{\hat{\mathbf{u}}}^*, \mathbf{h}_{\perp\hat{\mathbf{u}}}^*]) + \mathcal{V}_{\text{ext}}[\tilde{n}_{\hat{\mathbf{u}}}^*] + \mathcal{U}_H[\tilde{n}_{\hat{\mathbf{u}}}^*] + \mathcal{E}_{\text{xc}}[\tilde{n}_{\hat{\mathbf{u}}}^*] \\ &\quad - \int_V d^3\mathbf{r} \mathbf{m}_{\hat{\mathbf{u}}}^* \cdot \mathbf{h}_{\perp\hat{\mathbf{u}}}^*. \end{aligned} \quad (46)$$

The functional $\mathcal{E}_{\text{exch}}[\hat{\mathbf{u}}]$, or, equivalently, the torque density $\mathbf{\Gamma}_{\hat{\mathbf{u}}}(\mathbf{r})$, contains all the information we may wish to know about exchange interactions in the system.

B. Harris-Foulkes functional and “force theorems”

The self-consistent method described above constitute a conceptually straightforward approach for computing exchange interactions. However, this approach also has severe drawbacks.

- First of all, self-consistent calculations are computationally very demanding, because a large number of iterations are usually required to achieve convergence towards the self-consistent solution with sufficient accuracy.

- Second, within the self-consistent approach the exchange energy, which is typically of the order of 10^{-4} to 10^{-3} eV/atom, is obtained as the difference between the total energies for two different configurations, which are of the order of 10^4 eV/atom; thus, the total energies must be obtained with a tremendous relative accuracy in order to get reliable results. In this case, the results may be plagued by roundoff errors.
- But the most serious difficulty we face when using the self-consistent approach is that it provides us very little physical insight about the mechanism of exchange interaction.

For all the reasons mentioned above, it is desirable to develop a method which is computationally convenient and accurate, and at the same provides a clear physical picture of the mechanism of exchange interaction. The fact the energy of exchange interactions is small as compared to the total energy of the system suggests us that a perturbation-like theory might be appropriate. Alternatively, one can exploit the variational properties of the density functional to compute approximately the constrained ground state energy in a single non-self-consistent shoot. This the approach we shall adopt here. We shall derive a force theorem [100,101] that allows to express $\mathcal{E}_{\text{exch}}[\hat{\mathbf{u}}]$ (within an unimportant constant) in terms of the sum of single-particle energies, calculated non-self-consistently.

Because of its variational property of the energy functional $\mathcal{F}_{\hat{\mathbf{u}}}[\tilde{n}, \mathbf{h}_{\perp\hat{\mathbf{u}}}]$ satisfies

$$\mathcal{F}_{\hat{\mathbf{u}}}[\tilde{n}, \mathbf{h}_{\perp\hat{\mathbf{u}}}] = \mathcal{E}_{\text{exch}}[\hat{\mathbf{u}}] + \mathcal{O}_2(\tilde{n} - \tilde{n}_{\hat{\mathbf{u}}}^*, \mathbf{h}_{\perp\hat{\mathbf{u}}} - \mathbf{h}_{\perp\hat{\mathbf{u}}}^*) \quad (47)$$

where $\mathcal{O}_2(\tilde{n} - \tilde{n}_{\hat{\mathbf{u}}}^*, \mathbf{h}_{\perp\hat{\mathbf{u}}} - \mathbf{h}_{\perp\hat{\mathbf{u}}}^*)$ is of second order with respect to $\tilde{n} - \tilde{n}_{\hat{\mathbf{u}}}^*$ and $\mathbf{h}_{\perp\hat{\mathbf{u}}} - \mathbf{h}_{\perp\hat{\mathbf{u}}}^*$. So, if we have good guesses \tilde{n} and $\mathbf{h}_{\perp\hat{\mathbf{u}}}$ for the exact $\tilde{n}_{\hat{\mathbf{u}}}^*$ and $\mathbf{h}_{\perp\hat{\mathbf{u}}}^*$, and if we are able to compute $\mathcal{F}_{\hat{\mathbf{u}}}[\tilde{n}, \mathbf{h}_{\perp\hat{\mathbf{u}}}]$, we get an estimate of $\mathcal{E}_{\text{exch}}[\hat{\mathbf{u}}]$ which is accurate to second order in the error of our initial guesses. As we shall see just below, the difficulty of this approach lies in the calculation of $\mathcal{F}_{\hat{\mathbf{u}}}[\tilde{n}, \mathbf{h}_{\perp\hat{\mathbf{u}}}]$ for the chosen \tilde{n} and $\mathbf{h}_{\perp\hat{\mathbf{u}}}$.

This is seen as follows. From a trial input density \tilde{n}_{in} and input transverse field $\mathbf{h}_{\perp\hat{\mathbf{u}}}^{\text{in}}$ one gets the effective potential spinor $\tilde{w}_{\text{eff}}[\tilde{n}_{\text{in}}, \mathbf{h}_{\perp\hat{\mathbf{u}}}^{\text{in}}]$; by solving the Kohn-Sham equations for this effective potential spinor one gets a set of single particle energies $\varepsilon_i[\tilde{n}_{\text{in}}, \mathbf{h}_{\perp\hat{\mathbf{u}}}^{\text{in}}]$, from which one can in turn compute an output density \tilde{n}_{out} . From this, we can compute

$$\begin{aligned} \mathcal{F}_{\hat{\mathbf{u}}}[\tilde{n}_{\text{out}}, \mathbf{h}_{\perp\hat{\mathbf{u}}}^{\text{in}}] &= \sum_{\varepsilon_i \leq \varepsilon_F} \varepsilon_i[\tilde{n}_{\text{in}}, \mathbf{h}_{\perp\hat{\mathbf{u}}}^{\text{in}}] - \int d^3\mathbf{r} \text{tr} \left(\tilde{n}_{\text{out}} \tilde{w}_{\text{eff}}[\tilde{n}_{\text{in}}, \mathbf{h}_{\perp\hat{\mathbf{u}}}^{\text{in}}] \right) \\ &+ \mathcal{V}_{\text{ext}}[\tilde{n}_{\text{out}}] + \mathcal{U}_H[\tilde{n}_{\text{out}}] + \mathcal{E}_{\text{xc}}[\tilde{n}_{\text{out}}] - \int_V d^3\mathbf{r} \mathbf{m}_{\text{out}} \cdot \mathbf{h}_{\perp\hat{\mathbf{u}}}^{\text{in}} \end{aligned} \quad (48)$$

We now see where the problem lies: we get an estimate of the energy functional corresponding to the output density spinor, not to the input one; furthermore, the expression mixes in a complicated manner \tilde{n}_{in} and \tilde{n}_{out} . Since we don't know the input density spinor corresponding to an arbitrary output density spinor, this cannot be used to compute the energy functional for a chosen density spinor.

This problem was circumvented by Harris [102] who defined an auxiliary functional as follows

$$\begin{aligned} \mathcal{G}_{\hat{\mathbf{u}}}[\tilde{n}_{\text{in}}, \tilde{w}_{\text{in}}, \mathbf{h}_{\perp\hat{\mathbf{u}}}^{\text{in}}] \equiv & \sum_{\varepsilon_i \leq \varepsilon_F} \varepsilon_i[\tilde{w}_{\text{in}}] - \int d^3\mathbf{r} \text{tr}(\tilde{n}_{\text{in}} \tilde{w}_{\text{in}}) + \mathcal{V}_{\text{ext}}[\tilde{n}_{\text{in}}] + \mathcal{U}_H[\tilde{n}_{\text{in}}] + \mathcal{E}_{\text{xc}}[\tilde{n}_{\text{in}}] \\ & - \int_V d^3\mathbf{r} \mathbf{m}_{\text{in}} \cdot \mathbf{h}_{\perp\hat{\mathbf{u}}}^{\text{in}} \end{aligned} \quad (49)$$

where \tilde{n}_{in} is the input density, $\varepsilon_i[\tilde{w}_{\text{in}}]$ are the single particle energies calculated with the input effective potential \tilde{w}_{in} , and $\mathbf{h}_{\perp\hat{\mathbf{u}}}^{\text{in}}$ is the input transverse field. Here we have used a generalization of the Harris functional proposed by Foulkes and Haydock [103]. It is straightforward to show that

$$\mathcal{G}_{\hat{\mathbf{u}}}[\tilde{n}, \tilde{w}, \mathbf{h}_{\perp\hat{\mathbf{u}}}] = \mathcal{F}_{\hat{\mathbf{u}}}[\tilde{n}_{\hat{\mathbf{u}}}^*, \mathbf{h}_{\perp\hat{\mathbf{u}}}^*] + \mathcal{O}_2(\tilde{n} - \tilde{n}_{\hat{\mathbf{u}}}^*, \tilde{w} - \tilde{w}_{\hat{\mathbf{u}}}^*, \mathbf{h}_{\perp\hat{\mathbf{u}}} - \mathbf{h}_{\perp\hat{\mathbf{u}}}^*) \quad (50)$$

where

$$\tilde{w}_{\hat{\mathbf{u}}}^* \equiv \tilde{w}_{\text{ext}} + \tilde{w}_H[\tilde{n}_{\hat{\mathbf{u}}}^*] + \tilde{w}_{\text{xc}}[\tilde{n}_{\hat{\mathbf{u}}}^*] - \mathbf{h}_{\perp\hat{\mathbf{u}}}^* \cdot \tilde{\boldsymbol{\sigma}} \quad (51)$$

and $\mathcal{O}_2(\tilde{n} - \tilde{n}_{\hat{\mathbf{u}}}^*, \tilde{w} - \tilde{w}_{\hat{\mathbf{u}}}^*, \mathbf{h}_{\perp\hat{\mathbf{u}}} - \mathbf{h}_{\perp\hat{\mathbf{u}}}^*)$ is a (non generally positive) error of second order with respect $\tilde{n} - \tilde{n}_{\hat{\mathbf{u}}}^*$, $\tilde{w} - \tilde{w}_{\hat{\mathbf{u}}}^*$ and $\mathbf{h}_{\perp\hat{\mathbf{u}}} - \mathbf{h}_{\perp\hat{\mathbf{u}}}^*$. The properties of the Harris functionals have been discussed by a number of authors [104–106] who found that it often yields better approximate estimations of the ground state energy than the Hohenberg-Kohn functional.

We now have all the material needed to establish the force theorem for magnetic exchange interactions. To this end, we make the following choice for the input values of \tilde{n} , \tilde{w} and $\mathbf{h}_{\perp\hat{\mathbf{u}}}$:

$$\tilde{n}_{\text{in}}(\mathbf{r}) = \frac{\rho_{\text{in}}(\mathbf{r}) \tilde{\sigma}_0 + m_{\text{in}}(\mathbf{r}) \hat{\mathbf{u}}(\mathbf{r}) \cdot \tilde{\boldsymbol{\sigma}}}{2} \quad (52a)$$

$$\mathbf{h}_{\perp\hat{\mathbf{u}}}^{\text{in}}(\mathbf{r}) = 0 \quad (52b)$$

$$\tilde{w}_{\text{in}}(\mathbf{r}) = v_{\text{in}}(\mathbf{r}) \tilde{\sigma}_0 - h_{\text{in}}(\mathbf{r}) \hat{\mathbf{u}}(\mathbf{r}) \cdot \tilde{\boldsymbol{\sigma}}. \quad (52c)$$

The input charge and spin densities are chosen to be independent of $\hat{\mathbf{u}}$ in magnitude, with the axis of the spin-polarization along $\hat{\mathbf{u}}$; thus we neglect the redistribution of charge and magnetic moment due to rotating the magnetic moments, which usually constitutes a good approximation. The input effective field is chosen to be parallel to $\hat{\mathbf{u}}$; this is usually a good approximation, because the transverse component of the effective field is much smaller than its longitudinal component, which is of the order of the exchange splitting.

For the magnitude of the input effective potential v_{in} and input effective field h_{in} we can specify a little more by ascribing them the value corresponding to the LDA, i.e.,

$$v_{\text{in}}(\mathbf{r}) = v_{\text{ext}}(\mathbf{r}) + v_H[\rho_{\text{in}}](\mathbf{r}) + v_{\text{xc}}^{\text{LDA}}[\rho_{\text{in}}, m_{\text{in}}](\mathbf{r}) \quad (53a)$$

$$h_{\text{in}}(\mathbf{r}) = h_{\text{xc}}^{\text{LDA}}[\rho_{\text{in}}, m_{\text{in}}](\mathbf{r}). \quad (53b)$$

However, this choice is not necessary and the stationarity of the Harris functional allows more flexibility in the choice of the input values for the effective potential and effective field.

Inserting the particular choice (52a,b,c) for the input quantities in the definition of the Harris functional (49) we find

$$\begin{aligned} \mathcal{G}_{\hat{\mathbf{u}}}[\tilde{n}_{\text{in}}, \tilde{w}_{\text{in}}, \mathbf{h}_{\perp\hat{\mathbf{u}}}^{\text{in}}] &\equiv \sum_{\varepsilon_i \leq \varepsilon_F} \varepsilon_i[v_{\text{in}}, h_{\text{in}}\hat{\mathbf{u}}] - \int d^3\mathbf{r} (\rho_{\text{in}}v_{\text{in}} - m_{\text{in}}h_{\text{in}}) \\ &+ \mathcal{V}_{\text{ext}}[\rho_{\text{in}}] + \mathcal{U}_H[\rho_{\text{in}}] + \mathcal{E}_{\text{xc}}[\rho_{\text{in}}, m_{\text{in}}]. \end{aligned} \quad (54)$$

We find that the only term which depends on the constraint $\hat{\mathbf{u}}$ is the sum of single particle energies. Thus, we finally obtain

$$\begin{aligned} \mathcal{E}_{\text{exch}}[\hat{\mathbf{u}}_1] - \mathcal{E}_{\text{exch}}[\hat{\mathbf{u}}_2] &= \sum_{\varepsilon_i \leq \varepsilon_F} \varepsilon_i[v_{\text{in}}, h_{\text{in}}\hat{\mathbf{u}}_1] - \sum_{\varepsilon_i \leq \varepsilon_F} \varepsilon_i[v_{\text{in}}, h_{\text{in}}\hat{\mathbf{u}}_2] \\ &+ \mathcal{O}_2(\rho_{\text{in}} - \rho_{\hat{\mathbf{u}}}^*, m_{\text{in}} - m_{\hat{\mathbf{u}}}^*, \mathbf{h}_{\perp\hat{\mathbf{u}}}^*) \end{aligned} \quad (55)$$

which constitutes the force theorem for the exchange interaction energy. This is an important result, for several reasons:

- The energy of exchange interactions $\mathcal{E}_{\text{exch}}[\hat{\mathbf{u}}]$ can be computed (within an unimportant constant) in a single shoot, without need for lengthy iterations towards self-consistency, which makes the calculations considerably faster and easier.
- Although the exchange energy is ultimately due to Coulomb interactions between electrons, it is expressed here as a sum of single-particle energies for independent electrons. This is of considerable practical importance, because the sum of single particle energies is much smaller than the total energy of the system; thus the relative accuracy needed is much less than for self-consistent total energy calculations, and the risk of computational error is much smaller.
- A further remarkable feature of this result is that the exchange energy difference depends only on the input potential and input field, and not at all on the input charge and spin densities (as long as the latter don't vary much upon rotating the moments). This leaves considerable flexibility in setting up practical computational schemes, and allows to use suitably parametrized schemes, without jeopardizing seriously the accuracy of the results.

The torque density is given by

$$\begin{aligned} \mathbf{\Gamma}_{\hat{\mathbf{u}}}(\mathbf{r}) &\equiv - \frac{\delta \mathcal{E}_{\text{exch}}[\hat{\mathbf{u}}]}{\delta \mathbf{\Omega}(\mathbf{r})} \\ &\approx - \sum_{\varepsilon_i \leq \varepsilon_F} \frac{\delta \varepsilon_i[\hat{\mathbf{u}}]}{\delta \mathbf{\Omega}(\mathbf{r})}. \end{aligned} \quad (56)$$

From the Hellman-Feynman theorem, we obtain for a given single-particle energy $\varepsilon_i[\hat{\mathbf{u}}]$ corresponding to the wave function $|\phi_i[\hat{\mathbf{u}}]\rangle$,

$$\frac{\delta \varepsilon_i[\hat{\mathbf{u}}]}{\delta \mathbf{\Omega}(\mathbf{r})} = \langle \phi_i[\hat{\mathbf{u}}] | \frac{\delta H}{\delta \mathbf{\Omega}(\mathbf{r})} | \phi_i[\hat{\mathbf{u}}] \rangle. \quad (57)$$

Upon performing the rotation $\mathbf{\Omega}(\mathbf{r}) \equiv \Omega(\mathbf{r}) \mathbf{n}_{\Omega}(\mathbf{r})$, which changes $\hat{\mathbf{u}}(\mathbf{r})$ into $\hat{\mathbf{u}}'(\mathbf{r})$, the effective potential $\tilde{w}_{\text{eff}}(\mathbf{r})$ is transformed according to (for simplicity, the subscript “eff” will be omitted below)

$$\tilde{w}_{\hat{\mathbf{u}}}(\mathbf{r}) \rightarrow \tilde{w}_{\hat{\mathbf{u}}'}(\mathbf{r}) = \tilde{R}(\mathbf{r}) \tilde{w}_{\hat{\mathbf{u}}}(\mathbf{r}) \tilde{R}^{-1}(\mathbf{r}) \quad (58)$$

where the rotation matrix is given by

$$\begin{aligned} \tilde{R}(\mathbf{r}) &\equiv e^{-i\mathbf{\Omega}(\mathbf{r}) \cdot \tilde{\boldsymbol{\sigma}}} \\ &= \cos\left(\frac{\Omega(\mathbf{r})}{2}\right) - i \mathbf{n}_{\Omega}(\mathbf{r}) \Omega(\mathbf{r}) \cdot \tilde{\boldsymbol{\sigma}} \sin\left(\frac{\Omega(\mathbf{r})}{2}\right). \end{aligned} \quad (59)$$

Thus,

$$\frac{\delta H}{\delta \mathbf{\Omega}(\mathbf{r})} = - |\mathbf{r}\rangle h_{\text{in}}(\mathbf{r}) \hat{\mathbf{u}} \cdot \tilde{\boldsymbol{\sigma}} \langle \mathbf{r}| \quad (60)$$

and by using the relation

$$\mathbf{m}_{\text{out}}(\mathbf{r}) = \sum_{\varepsilon_i \leq \varepsilon_F} \langle \phi_i[\hat{\mathbf{u}}] | \mathbf{r} \rangle \tilde{\boldsymbol{\sigma}} \langle \mathbf{r} | \phi_i[\hat{\mathbf{u}}] \rangle \quad (61)$$

we finally obtain

$$\mathbf{\Gamma}_{\hat{\mathbf{u}}}(\mathbf{r}) = - h_{\text{in}}(\mathbf{r}) \hat{\mathbf{u}} \times \mathbf{m}_{\text{out}}(\mathbf{r}). \quad (62)$$

The above result constitutes the force theorem for the exchange torque density.

C. Examples of first-principles calculations of IEC

The use of the magnetic “force theorems” discussed in the preceding Section allows to reduce by several orders of magnitude the computation times required to calculate the interlayer exchange coupling. Such first-principles calculations have been performed by a number of authors [18–30].

The Fig. 11 shows the interlayer exchange coupling for the Co/Cu/Co(001) systems, for semi-infinite Co layers (top), and 5 AL thick Co layers (bottom) [107]. The data have been multiplied by N^2 in order to highlight the $1/N^2$ dependence of the IEC, as predicted from the asymptotic approximation. The data corresponding to the two different Co thicknesses seem very different at first sight. In order to evidence more clearly the periodic oscillatory behavior, one can perform a discrete Fourier analysis of the N dependence of the IEC [21]. The corresponding results are shown in Fig. 12.

One sees very clearly that the oscillations comprise two superimposed oscillatory components, as expected, with periods in good agreement with the ones predicted in terms of the spacer Fermi surface [4]. On the other hand the amplitude of the oscillations change dramatically, as the Co thickness is varied.

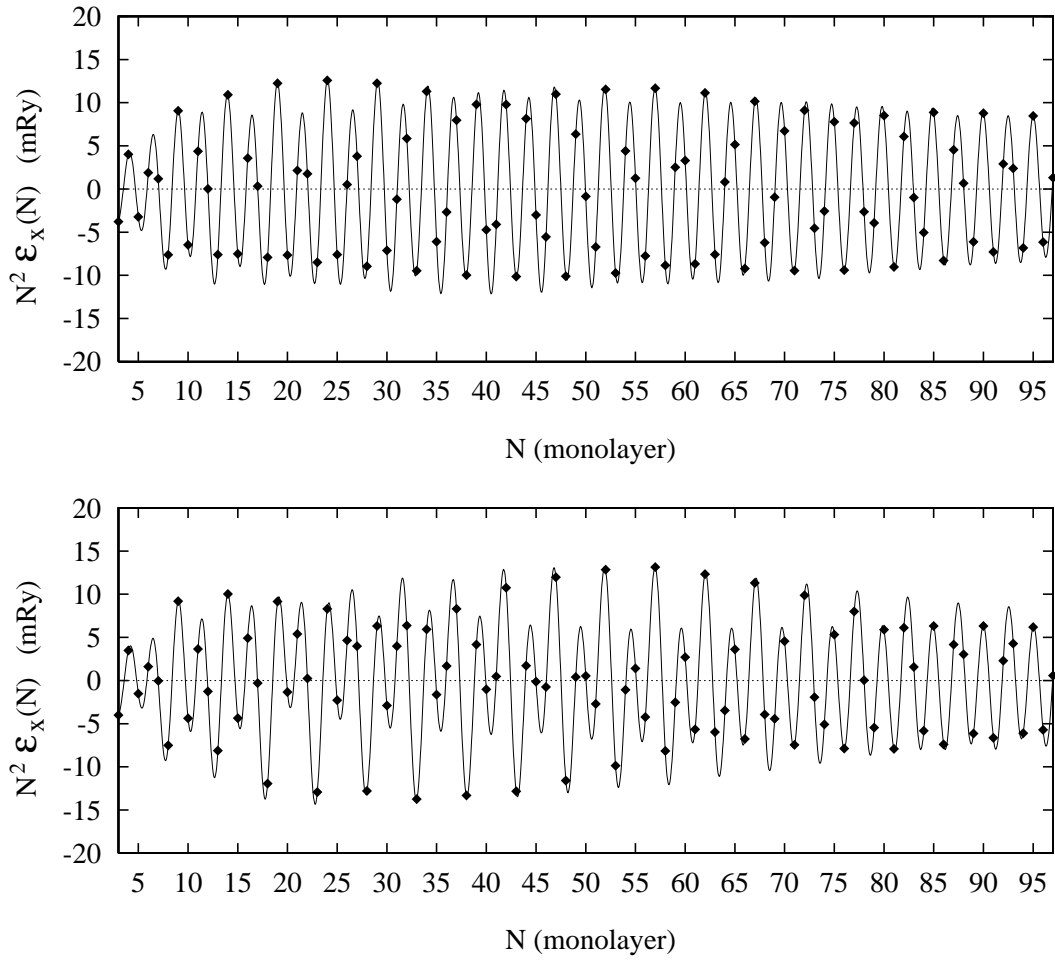


FIG. 11. Calculated interlayer exchange coupling $N^2 \mathcal{E}_x$ as a function of spacer thickness N (in AL) for the Co/Cu/Co(001) system; top panel: semi-infinite Co layers; bottom panel: 5 AL thick Co layers [107].

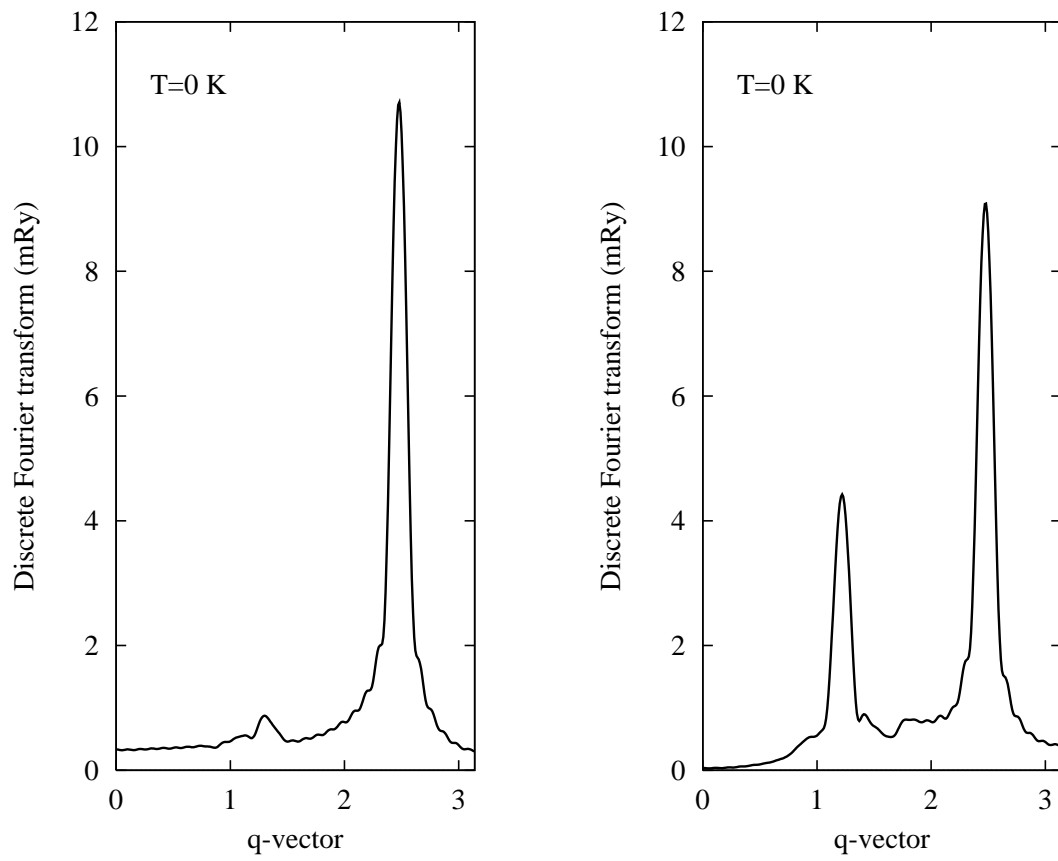


FIG. 12. Discrete Fourier transform of the data shown in Fig. 11; left panel: semi-infinite Co layers; right panel: 5 AL thick Co layers [107].

These results provide a very clear confirmation of the results obtained from the discussion in terms of quantum interferences in the asymptotic regime, namely that the periods of oscillation versus spacer thickness depend only on the spacer material, but the amplitudes can vary with the thickness (as in the present case) or nature of the ferromagnetic layers.

IV. SUBSTITUTIONAL DISORDER

The case where (some part of) the system under consideration consists of a substitutionally disordered alloys is extremely important in practice. This happens of course if some layers are *by purpose* chosen to consist of alloy; but more generally, unavoidable interdiffusion takes place at the interfaces, giving rise to a disordered interface region with a progressive variation of concentration.

A. “Vertex cancellation” theorem

We present here a general discussion of exchange interactions in the presence of substitutional disorder. The results given here are used in the present paper to study interlayer exchange interactions, but they are also applicable for studying exchange interactions *within* a ferromagnet, exchange stiffnesses, spin-wave energies, etc.

The principal result is the “vertex cancellation theorem” of Bruno *et al.* [108]. We present here an alternative, more general, derivation of this result.

Let us specify the notations used here. Our purpose is to compute the total energy (more precisely the thermodynamic grand-potential) as a function of the prescribed local direction $\hat{\mathbf{u}}(\mathbf{r})$ of the magnetization. Explicitly, the Hamiltonian operator corresponding to a particular configuration $\hat{\mathbf{u}} \equiv \{\hat{\mathbf{u}}(\mathbf{r})\}$ of the local moments is written as

$$\mathbf{H} = \mathbf{K} + \mathbf{V}_{\hat{\mathbf{u}}}. \quad (63)$$

The matrix elements of the kinetic energy operator \mathbf{K} are

$$\langle \mathbf{r} | \mathbf{K} | \mathbf{r}' \rangle \equiv \delta(\mathbf{r} - \mathbf{r}') \frac{-\hbar^2}{2m} \frac{d^2}{d\mathbf{r}^2} \tilde{\sigma}_0, \quad (64)$$

and those of the potential operator \mathbf{V}

$$\langle \mathbf{r} | \mathbf{V}_{\hat{\mathbf{u}}} | \mathbf{r}' \rangle \equiv \delta(\mathbf{r} - \mathbf{r}') [v(\mathbf{r}) \tilde{\sigma}_0 - h(\mathbf{r}) \hat{\mathbf{u}}(\mathbf{r}) \cdot \tilde{\boldsymbol{\sigma}}], \quad (65)$$

where $v(\mathbf{r})$ and $h(\mathbf{r})$ are respectively the local effective potential and the local effective field. The corresponding Green’s function operator is

$$\mathbf{G}_{\hat{\mathbf{u}}}(z) \equiv (z - \mathbf{H}_{\hat{\mathbf{u}}})^{-1}. \quad (66)$$

Because of the substitutional disorder, $v(\mathbf{r})$ and $h(\mathbf{r})$ have some spacial randomness. However, within the domain of applicability of the “force theorem”, we assume that they are unchanged upon changing the moment configuration $\hat{\mathbf{u}}$.

The central quantity in the theory of disordered alloys is the *configuration averaged* Green’s function

$$\overline{\mathbf{G}}_{\hat{\mathbf{u}}}(z) \equiv \langle \mathbf{G}_{\hat{\mathbf{u}}}(z) \rangle_c \equiv [z - \mathbf{K} - \Sigma_{\hat{\mathbf{u}}}(z)]^{-1} \quad (67)$$

where $\langle \dots \rangle_c$ indicates an average over all possible alloy configurations, and where $\Sigma_{\hat{\mathbf{u}}}(z)$ is the self-energy. The Green’s function is given by

$$\mathbf{G}_{\hat{\mathbf{u}}}(z) = \overline{\mathbf{G}}_{\hat{\mathbf{u}}}(z) + \overline{\mathbf{G}}_{\hat{\mathbf{u}}}(z) \mathbf{T}_{\hat{\mathbf{u}}}(z) \overline{\mathbf{G}}_{\hat{\mathbf{u}}}(z), \quad (68)$$

where the t-matrix $\mathbf{T}_{\hat{\mathbf{u}}}(z)$ is given by

$$\mathbf{T}_{\hat{\mathbf{u}}}(z) \equiv (\mathbf{V}_{\hat{\mathbf{u}}} - \Sigma_{\hat{\mathbf{u}}}(z)) \left[1 - \overline{\mathbf{G}}_{\hat{\mathbf{u}}}(z) (\mathbf{V}_{\hat{\mathbf{u}}} - \Sigma_{\hat{\mathbf{u}}}(z)) \right]^{-1}. \quad (69)$$

From the definition of the configuration averaged green’s function, we get the self-consistency condition

$$\langle \mathbf{T}_{\hat{\mathbf{u}}}(z) \rangle_c = 0, \quad (70)$$

or equivalently,

$$\left\langle \left[1 - \overline{\mathbf{G}}_{\hat{\mathbf{u}}}(z) (\mathbf{V}_{\hat{\mathbf{u}}} - \Sigma_{\hat{\mathbf{u}}}(z)) \right]^{-1} \right\rangle_c = 1. \quad (71)$$

In practice, the self-energy satisfying the conditions (70, 71) cannot be calculated exactly and one has to resort to approximations. The most popular approach is the CPA, in which conditions (70, 71) are replaced by *on site* conditions, for all atomic sites \mathbf{R} .

If one uses the “force theorem”, the thermodynamic grand-potential includes only the single-particle energies (Kohn-Sham eigenvalues) and is given by

$$\Phi_{\hat{\mathbf{u}}} = - \int_{-\infty}^{+\infty} d\varepsilon f(\varepsilon) N_{\hat{\mathbf{u}}}(\varepsilon), \quad (72)$$

where $f(\varepsilon)$ is the Fermi-Dirac function, and $N_{\hat{\mathbf{u}}}(\varepsilon)$ the integrated density of states (averaged over all possible alloy configurations) for the local moment configuration $\hat{\mathbf{u}}$. The integrated density of states is given by

$$N_{\hat{\mathbf{u}}}(\varepsilon) = \frac{1}{\pi} \text{Im} \text{Tr} [\langle \ln \mathbf{G}(z) \rangle_c]_{z=\varepsilon+i0^+}^{z=-\infty+i0^+}. \quad (73)$$

Let us consider the quantity

$$A_{\hat{\mathbf{u}}}(z) \equiv \text{Tr} \langle \ln \mathbf{G}_{\hat{\mathbf{u}}}(z) \rangle_c. \quad (74)$$

By some simple algebra, one can show that

$$A_{\hat{\mathbf{u}}}(z) = \text{Tr} \left[\ln \bar{\mathbf{G}}_{\hat{\mathbf{u}}}(z) \right] - X_{\hat{\mathbf{u}}}(z) \quad (75)$$

where

$$X_{\hat{\mathbf{u}}}(z) \equiv \text{Tr} \left\langle \ln [1 - \mathbf{G}_{\hat{\mathbf{u}}}(z) (\mathbf{V}_{\hat{\mathbf{u}}} - \Sigma_{\hat{\mathbf{u}}}(z))] \right\rangle_c \quad (76)$$

is called the *vertex correction*. This term is usually non negligible and is difficult to calculate. We shall show however that its variation upon varying $\hat{\mathbf{u}}$ takes a simple form.

Let us precise the variation of the Hamiltonian under varying $\hat{\mathbf{u}}$. If we chose a reference configuration $\hat{\mathbf{u}}_0$ for the local moment configuration, the configuration $\hat{\mathbf{u}}$ is obtained by performing locally a rotation of vector

$$\boldsymbol{\Omega}(\mathbf{r}) \equiv \Omega(\mathbf{r}) \hat{\mathbf{n}}_{\Omega}(\mathbf{r}). \quad (77)$$

Explicitly, one has

$$\hat{\mathbf{u}} \equiv (\hat{\mathbf{n}}_{\Omega} \cdot \hat{\mathbf{u}}_0) \hat{\mathbf{n}}_{\Omega} + \cos \Omega (\hat{\mathbf{n}}_{\Omega} \times \hat{\mathbf{u}}) \times \hat{\mathbf{n}}_{\Omega} + \sin \Omega (\hat{\mathbf{n}}_{\Omega} \times \hat{\mathbf{u}}). \quad (78)$$

The potential operator $\mathbf{V}_{\hat{\mathbf{u}}}$ corresponding to $\hat{\mathbf{u}}$ is obtained from $\mathbf{V}_{\hat{\mathbf{u}}_0}$ as

$$\mathbf{V}_{\hat{\mathbf{u}}} \equiv \mathbf{R}_{\Omega} \mathbf{V}_{\hat{\mathbf{u}}_0} \mathbf{R}_{\Omega}^{-1}, \quad (79)$$

and the matrix elements of the rotation operator \mathbf{R}_{Ω} are given by

$$\begin{aligned} \langle \mathbf{r} | \mathbf{R}_{\Omega} | \mathbf{r}' \rangle &\equiv \delta(\mathbf{r} - \mathbf{r}') \exp \left(-\frac{i}{2} \boldsymbol{\Omega}(\mathbf{r}) \cdot \tilde{\boldsymbol{\sigma}} \right) \\ &= \delta(\mathbf{r} - \mathbf{r}') \left[\cos \left(\frac{\Omega(\mathbf{r})}{2} \right) \tilde{\sigma}_0 - i \sin \left(\frac{\Omega(\mathbf{r})}{2} \right) \hat{\mathbf{n}}_{\Omega}(\mathbf{r}) \cdot \tilde{\boldsymbol{\sigma}} \right]. \end{aligned} \quad (80)$$

We shall also make of the relation

$$\frac{\delta (\mathbf{R}_{\Omega} \mathbf{B} \mathbf{R}_{\Omega}^{-1})}{\delta \boldsymbol{\Omega}(\mathbf{r})} = -\frac{i}{2} [|\mathbf{r}\rangle \tilde{\boldsymbol{\sigma}} \langle \mathbf{r}| ; \mathbf{R}_{\Omega} \mathbf{B} \mathbf{R}_{\Omega}^{-1}]_-, \quad (81)$$

for an arbitrary operator \mathbf{B} .

The derivative of $A_{\hat{\mathbf{u}}}$ (from now on, we shall omit the dependence on complex energy z) with respect to $\boldsymbol{\Omega}$ is given by

$$\frac{\delta A_{\hat{\mathbf{u}}}}{\delta \boldsymbol{\Omega}(\mathbf{r})} = \text{Tr} \left[\bar{\mathbf{G}}_{\hat{\mathbf{u}}} \frac{\delta \Sigma_{\hat{\mathbf{u}}}}{\delta \boldsymbol{\Omega}(\mathbf{r})} \right] - \frac{\delta X_{\hat{\mathbf{u}}}}{\delta \boldsymbol{\Omega}(\mathbf{r})}, \quad (82)$$

with

$$\begin{aligned} \frac{\delta X_{\hat{\mathbf{u}}}}{\delta \boldsymbol{\Omega}(\mathbf{r})} &= -\text{Tr} \left[\frac{\delta \bar{\mathbf{G}}_{\hat{\mathbf{u}}}}{\delta \boldsymbol{\Omega}(\mathbf{r})} \left\langle (\mathbf{V}_{\hat{\mathbf{u}}} - \Sigma_{\hat{\mathbf{u}}}) [1 - \bar{\mathbf{G}}_{\hat{\mathbf{u}}} (\mathbf{V}_{\hat{\mathbf{u}}} - \Sigma_{\hat{\mathbf{u}}})]^{-1} \right\rangle_c \right] \\ &\quad - \text{Tr} \left\langle \bar{\mathbf{G}}_{\hat{\mathbf{u}}} \left(\frac{\delta \mathbf{V}_{\hat{\mathbf{u}}}}{\delta \boldsymbol{\Omega}(\mathbf{r})} - \frac{\delta \Sigma_{\hat{\mathbf{u}}}}{\delta \boldsymbol{\Omega}(\mathbf{r})} \right) [1 - \bar{\mathbf{G}}_{\hat{\mathbf{u}}} (\mathbf{V}_{\hat{\mathbf{u}}} - \Sigma_{\hat{\mathbf{u}}})]^{-1} \right\rangle_c. \end{aligned} \quad (83)$$

The first term on the right-hand side of the above equation is zero, because of condition (70). Next, we split the self-energy in two parts as

$$\Sigma_{\hat{\mathbf{u}}} \equiv \Sigma_{\hat{\mathbf{u}}}^{(1)} + \Sigma_{\hat{\mathbf{u}}}^{(2)}, \quad (84)$$

where $\Sigma_{\hat{\mathbf{u}}}^{(1)}$ varies with Ω like $V_{\hat{\mathbf{u}}}$, i.e.,

$$\Sigma_{\hat{\mathbf{u}}}^{(1)} \equiv R_{\Omega} \Sigma_{\hat{\mathbf{u}}_0} R_{\Omega}^{-1}. \quad (85)$$

Then, we obtain

$$\begin{aligned} \frac{\delta X_{\hat{\mathbf{u}}}}{\delta \Omega(\mathbf{r})} &= \text{Tr} \left[\bar{\mathbf{G}}_{\hat{\mathbf{u}}} \frac{\delta \Sigma_{\hat{\mathbf{u}}}^{(2)}}{\delta \Omega(\mathbf{r})} \left\langle [1 - \bar{\mathbf{G}}_{\hat{\mathbf{u}}} (V_{\hat{\mathbf{u}}} - \Sigma_{\hat{\mathbf{u}}})]^{-1} \right\rangle_c \right] \\ &\quad - \text{Tr} \left\langle \bar{\mathbf{G}}_{\hat{\mathbf{u}}} \frac{(-i)}{2} [|\mathbf{r}\rangle \boldsymbol{\sigma} \langle \mathbf{r}| ; (V_{\hat{\mathbf{u}}} - \Sigma_{\hat{\mathbf{u}}}^{(1)})_-] [1 - \bar{\mathbf{G}}_{\hat{\mathbf{u}}} (V_{\hat{\mathbf{u}}} - \Sigma_{\hat{\mathbf{u}}})]^{-1} \right\rangle_c \end{aligned} \quad (86)$$

By using the permutation invariance of the trace and the conditions (70, 71), we obtain finally

$$\frac{\delta X_{\hat{\mathbf{u}}}}{\delta \Omega(\mathbf{r})} = \text{Tr} \left[\bar{\mathbf{G}}_{\hat{\mathbf{u}}} \frac{\delta \Sigma_{\hat{\mathbf{u}}}^{(2)}}{\delta \Omega(\mathbf{r})} \right] \quad (87)$$

and hence

$$\frac{\delta A_{\hat{\mathbf{u}}}}{\delta \Omega(\mathbf{r})} = \text{Tr} \left[\bar{\mathbf{G}}_{\hat{\mathbf{u}}} \frac{\delta \Sigma_{\hat{\mathbf{u}}}^{(1)}}{\delta \Omega(\mathbf{r})} \right]. \quad (88)$$

Thus, the torque density due to the exchange interactions is given by

$$\begin{aligned} \Gamma_{\hat{\mathbf{u}}}(\mathbf{r}) &\equiv - \frac{\delta \Phi_{\hat{\mathbf{u}}}}{\delta \Omega(\mathbf{r})} \\ &= \frac{1}{\pi} \int_{-\infty}^{+\infty} f(\varepsilon) \text{Im} \text{Tr} \left[\bar{\mathbf{G}}_{\hat{\mathbf{u}}}(\varepsilon + i0^+) \frac{\delta \Sigma_{\hat{\mathbf{u}}}^{(1)}(\varepsilon + i0^+)}{\delta \Omega(\mathbf{r})} \right] d\varepsilon. \end{aligned} \quad (89)$$

This exact result constitutes the ‘‘vertex cancellation theorem’’ for the torque density. Its usefulness arises from the fact that the ‘‘vertex corrections’’ have been eliminated. A further important feature is that the exact torque is given in terms of the angular derivative of $\Sigma_{\hat{\mathbf{u}}}^{(1)}$ only, which is known explicitly because it follows the angular variation of $V_{\hat{\mathbf{u}}}$; the angular derivative of the remaining part of the self-energy, $\Sigma_{\hat{\mathbf{u}}}^{(2)}$, which cannot be calculated easily, has been eliminated.

In order to compute the difference of thermodynamic grand-potential between two local moment configurations $\hat{\mathbf{u}}_1$ and $\hat{\mathbf{u}}_2$, we use a theorem due to Ducastelle [109], which states that the thermodynamic grand-potential, considered as a functional $\tilde{\Phi}[\bar{\mathbf{G}}, \mathbf{V}]$ of the *independent* variables $\bar{\mathbf{G}}$ and \mathbf{V} , is stationary with respect to $\bar{\mathbf{G}}$ when the latter satisfies the self-consistency condition (70, 71). This means that a first-order error on $\bar{\mathbf{G}}_{\hat{\mathbf{u}}}$ gives only a second-order error on $\Phi_{\hat{\mathbf{u}}}$. Writing $\bar{\mathbf{G}}_{\hat{\mathbf{u}}}$ as

$$\overline{\mathbf{G}}_{\hat{\mathbf{u}}}(z) \equiv \overline{\mathbf{G}}_{\hat{\mathbf{u}}}^{(1)}(z) + \overline{\mathbf{G}}_{\hat{\mathbf{u}}}^{(2)}(z) \quad (90)$$

with

$$\overline{\mathbf{G}}_{\hat{\mathbf{u}}}^{(1)}(z) \equiv \left(z - \mathbf{K} - \Sigma_{\hat{\mathbf{u}}}^{(1)}(z) \right)^{-1}, \quad (91)$$

we take $\overline{\mathbf{G}}_{\hat{\mathbf{u}}}^{(1)}$ as a trial value for computing $\Phi_{\hat{\mathbf{u}}}$. This can be expected to be a good approximation, provided the condition

$$m(\mathbf{r}) \left| \frac{d\Omega}{d\mathbf{r}} \right| \ll k_F \rho(\mathbf{r}) \quad (92)$$

(where $\rho(\mathbf{r})$ and $m(\mathbf{r})$ are respectively the electron and spin densities) is satisfied. Replacing $\overline{\mathbf{G}}_{\hat{\mathbf{u}}}$ by $\overline{\mathbf{G}}_{\hat{\mathbf{u}}}^{(1)}$ in Eq. (89), we can now integrate over angles, and we get

$$\Phi_{\hat{\mathbf{u}}_1} - \Phi_{\hat{\mathbf{u}}_2} \approx -\frac{1}{\pi} \int_{-\infty}^{+\infty} f(\varepsilon) \text{Im Tr} \left[\ln \overline{\mathbf{G}}_{\hat{\mathbf{u}}_1}^{(1)}(\varepsilon + i0^+) - \ln \overline{\mathbf{G}}_{\hat{\mathbf{u}}_2}^{(1)}(\varepsilon + i0^+) \right], \quad (93)$$

which constitutes the ‘‘vertex cancellation theorem’’ for exchange energies. In the derivation of the ‘‘vertex cancellation theorem’’, we have made use of the exact self-consistency condition (70, 71); one can show also that the same result holds if one uses the approximate CPA self-consistency condition.

In the case of interlayer coupling, the condition (92) is satisfied even for large rotation angles, because $d\Omega/d\mathbf{r}$ differs from zero only in a region where $m(\mathbf{r})$ is negligible. This was confirmed by explicit numerical calculations in Ref. [108].

B. Numerical studies of IEC in presence of alloy disorder

The interlayer exchange coupling through a $\text{Cu}_{1-x}\text{Ni}_x$ spacer layer has been studied experimentally by several groups [84–86]. These authors have observed a decrease of oscillation periods with increasing Ni concentration, which they have attributed to the shrinking of the Fermi surface.

First-principles calculations of IEC for the $\text{Co}/\text{Cu}_{1-x}\text{Ni}_x/\text{Co}(001)$, $\text{Co}/\text{Cu}_{1-x}\text{Zn}_x/\text{Co}(001)$, and $\text{Co}/\text{Cu}_{1-x}\text{Au}_x/\text{Co}(001)$ systems based upon the ‘‘vertex cancellation’’ theorem have been performed by Kudrnovský *et al.* [110]. Their results are shown in Fig. 13. The systematic shift of the oscillation periods with impurity concentration appears clearly. The decrease (resp. increase) of oscillation periods with increasing concentration of Ni (resp. Zn) is clearly due to decrease (resp. increase) number of conduction electrons. Alloying with an isoelectronic metal (Au) on the other, yields quasi-constant oscillation periods.

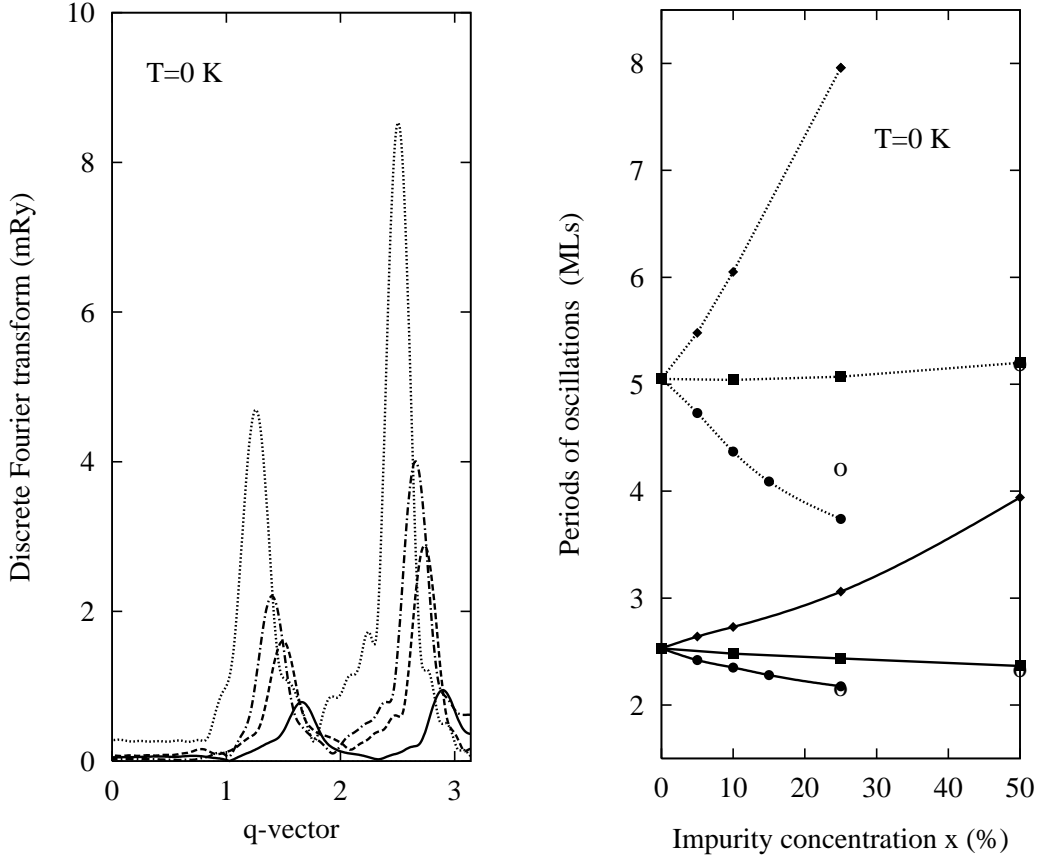


FIG. 13. Left panel: composition dependence of the absolute values of a discrete Fourier transform of \mathcal{E}_x at $T=0$ K for two Co(001) slabs each five monolayers thick separated by an fcc-Cu_{1-x}Ni_x alloy spacer: (i) Cu_{0.75}Ni_{0.25} (full line), (ii) Cu_{0.85}Ni_{0.15} (dashed line), Cu_{0.9}Ni_{0.1} (dashed-dotted line), and (iv) an ideal Cu spacer (dotted line); from Ref. [110]. Right panel: composition dependence of the coupling periods for two Co(001) slabs each five AL thick separated by an fcc-Cu_{1-x}M_x alloy spacer: (i) M=Ni (bullets), (ii) M=Au (squares), and (iii) M=Zn (diamonds). The lines serves as a guide for the eye and distinguish between short (full lines) and long (dotted lines) period oscillations. Open circles for Cu_{0.75}Ni_{0.25} and Cu_{0.5}Au_{0.5} represent the approximate virtual-crystal values. The periods are given in ALs; from Ref. [110].

REFERENCES

* Electronic address: `bruno@mpi-halle.de`

- [1] S.S.P. Parkin, N. More, and K.P. Roche, Phys. Rev. Lett. **64**, 2304 (1990).
- [2] Y. Yafet, Phys. Rev. B **36**, 3948 (1987).
- [3] C. Chappert and J.P. Renard, Europhys. Lett. **15**, 553 (1991).
- [4] P. Bruno and C. Chappert, Phys. Rev. Lett. **67**, 1602 (1991); **67**, 2592(E) (1991).
- [5] Phys. Rev. B **46**, 261 (1992).
- [6] R. Coehoorn, Phys. Rev. B **44**, 9331 (1991).
- [7] J. Barnaś, J. Magn. Magn. Mater. **111**, L215 (1992).
- [8] R.P. Erickson, K.B. Hathaway, and J.R. Cullen, Phys. Rev. B **47**, 2626 (1993).
- [9] J.C. Slonczewski, J. Magn. Magn. Mater. **126**, 374 (1993).
- [10] D.M. Edwards, J. Mathon, R.B. Muniz, and M.S. Phan, Phys. Rev. Lett. **67**, 493 (1991).
- [11] J. Mathon, M. Villeret, and D.M. Edwards, J. Phys. Condens. Mat. **4**, 9873 (1992).
- [12] Y. Wang, P.M. Levy, and J.L. Fry, Phys. Rev. Lett. **65**, 2732 (1990).
- [13] Z.P. Shi, P.M. Levy, and J.L. Fry, Phys. Rev. Lett. **69**, 3678 (1992).
- [14] P. Bruno, J. Magn. Magn. Mater. **116**, L13 (1992).
- [15] F. Herman, J. Sticht, and M. van Schilfhaarde, J. Appl. Phys. **69**, 4783 (1991); in *Magnetic Thin Films, Multilayers and Surfaces*, edited by S.S.P. Parkin, H. Hopster, J.P. Renard, T. Shinjo, and W. Zinn, Symposia Proceedings No. 231 (Materials Research Society, Pittsburg, 1992).
- [16] S. Krompiewski, U. Krey, and J. Pirnay, J. Magn. Magn. Mater. **121**, 238 (1993).
- [17] S. Krompiewski, F. Süß, and U. Krey, Europhys. Lett. **26**, 303 (1994).
- [18] M. van Schilfhaarde and F. Herman, Phys. Rev. Lett. **71**, 1923 (1993).
- [19] P. Lang, L. Nordström, R. Zeller, and P.H. Dederichs, Phys. Rev. Lett. **71**, 1927 (1993).
- [20] L. Norström, P. Lang, R. Zeller, and P.H. Dederichs, Phys. Rev. B **50**, 13058 (1994).
- [21] J. Kudrnovský, V. Drchal, I. Turek, and P. Weinberger, Phys. Rev. B **50**, 16105 (1994).
- [22] B. Lee and Y.-C. Chang, Phys. Rev. B **52**, 3499 (1995).

- [23] J. Kudrnovský, V. Drchal, I. Turek, M. Šob, and P. Weinberger, *Phys. Rev. B* **53**, 5125 (1996).
- [24] P. Lang, L. Nordström, K. Wildberger, R. Zeller, P.H. Dederichs, and T. Hoshino, *Phys. Rev. B* **53**, 9092 (1996).
- [25] V. Drchal, J. Kudrnovský, I. Turek, and P. Weinberger, *Phys. Rev. B* **53**, 15036 (1996).
- [26] M.D. Stiles, *J. Appl. Phys.* **79**, 5805 (1996).
- [27] J. d'Albuquerque e Castro, J. Mathon, M. Villeret, and A. Umerski, *Phys. Rev. B* **53**, R13306 (1996).
- [28] B. Lee and Y.C. Chang, *Phys. Rev. B* **54**, 13034 (1996).
- [29] J. Mathon, M. Villeret, A. Umerski, R.B. Muniz, J. d'Albuquerque e Castro, and D.M. Edwards, *Phys. Rev. B* **56**, 11797 (1997).
- [30] A.T. Costa, Jr., J. d'Albuquerque e Castro, and R.B. Muniz, *Phys. Rev. B* **56**, 13697 (1997).
- [31] P. Bruno, *J. Magn. Magn. Mater.* **121**, 248 (1993).
- [32] P. Bruno, *Phys. Rev. B* **52**, 411 (1995).
- [33] M.D. Stiles, *Phys. rev. B* **48** 7238 (1193).
- [34] P.D. Loly and J.B. Pendry, *J. Phys. C: Solid State Phys.* **16**, 423 (1983).
- [35] A.L. Wachs, A.P. Shapiro, T.C. Hsieh, and T.-C. Chiang, *Phys. Rev. B* **33**, 1460 (1986).
- [36] S.Å Lindgren and L. Walldén, *Phys. Rev. Lett.* **59**, 3003 (1987).
- [37] S.Å Lindgren and L. Walldén, *Phys. Rev. Lett.* **61**, 2894 (1988).
- [38] S.Å Lindgren and L. Walldén, *Phys. Rev. B* **38**, 3060 (1988).
- [39] S.Å Lindgren and L. Walldén, *J. Phys.: Condens. Matter* **1**, 2151 (1989).
- [40] T. Miller, A. Samsavar, G.E. Franklin, and T.-C. Chiang, *Phys. Rev. Lett.* **61**, 1404 (1988).
- [41] M.A. Mueller, A. Samsavar, T. Miller, and T.-C. Chiang, *Phys. Rev. B* **40**, 5845 (1989).
- [42] M.A. Mueller, T. Miller, and T.-C. Chiang, *Phys. Rev. B* **41**, 5214 (1990).
- [43] M. Jałochowski, E. Bauer, H. Knoppe, and G. Lilienkamp, *Phys. Rev. B* **45**, 13607 (1992).

- [44] N.B. Brookes, Y. Chang, and P.D. Johnson, Phys. Rev. Lett. **67**, 354 (1991).
- [45] J.E. Ortega and F.J. Himpsel, Phys. Rev. Lett. **69**, 844 1(992).
- [46] J.E. Ortega, F.J. Himpsel, G.J. Mankey, and R.F. Willis, Phys. Rev. B **47**, 1540 (1993).
- [47] J.E. Ortega, F.J. Himpsel, G.J. Mankey, and R.F. Willis, J. Appl. Phys. **73**, 5771 (1993).
- [48] K. Garrison, Y. Chang, and P.D. Johnson, Phys. Rev. Lett. **71**, 2801 (1993).
- [49] C. Carbone, E. Vescovo, O. Rader, W. Gudat, and W. Eberhardt, Phys. Rev. Lett. **71**, 2805 (1993).
- [50] N.V. Smith, N.B. Brookes, Y. Chang, and P.D. Johnson, Phys. Rev. B **49**, 332 (1994).
- [51] P.D. Johnson, K. Garrison, Q. Dong, N.V. Smith, D. Li, J. Mattson, J. Pearson, and S.D. Bader, Phys. Rev. B **50**, 8954 (1994).
- [52] F.J. Himpsel and O. Rader, Appl. Phys. Lett. **67**, 1151 (1995).
- [53] S. Crampin, S. De Rossi, and F. Ciccaci, Phys. Rev. B **53**, 13817 (1996).
- [54] P. Segovia, E.G. Michel, and J.E. Ortega, Phys. Rev. Lett. **77**, 3455 (1996).
- [55] R. Kläsge, D. Schmitz, C. Carbone, W. Eberhardt, P. Lang, R. Zeller, and P.H. Dederichs, Phys. Rev. B **57**, R696 (1998).
- [56] F.J. Himpsel, Phys. Rev. B **44**, 5966 (1991).
- [57] J.E. Ortega and F.J. Himpsel, Phys. Rev. B **47**, 16441 (1993).
- [58] D. Li, J. Pearson, J.E. Mattson, S.D. Bader, and P.D. Johnson, Phys. Rev. B **51**, 7195 (1995).
- [59] F.J. Himpsel, J. Electr. Microsc. and Rel. Phenom. **75**, 187 (1995).
- [60] D. Li, J. Pearson, S.D. Bader, E. Vescovo, D.-J. Huang, P.D. Johnson, and B. Heinrich, Phys. Rev. Lett. **78**, 1154 (1997).
- [61] K. Koike, T. Furukawa, G.P. Cameron, and Y. Murayama, Phys. Rev. B **50**, 4816 (1994).
- [62] T. Furukawa and K. Koike, Phys. Rev. B **54**, 17896 (1996).
- [63] W.R. Bennett, W. Schwarzacher, and W.F. Egelhoff, Jr., Phys. Rev. Lett. **65**, 3169 (1990).
- [64] T. Katayama, Y. Suzuki, M. Hayashi, and A. Thiaville, J. Magn. Magn. Mater. **126**,

527 (1993).

- [65] A. Carl and D. Weller, Phys. Rev. Lett. **74**, 190 (1995).
- [66] R. Mégy, A. Bounouh, Y. Suzuki, P. Beauvillain, P. Bruno, C. Chappert, B. Lécuyer, and P. Veillet, Phys. Rev. B **51**, 5586 (1995).
- [67] P. Bruno, Y. Suzuki and C. Chappert, Phys. Rev. B **53**, 9214 (1996).
- [68] Y. Suzuki, T. Katayama, P. Bruno, S. Yuasa, and E. Tamura, Phys. Rev. Lett. **80**, 5200 (1998).
- [69] T.A. Luce, W. Hübner, and K.H. Bennemann, Phys. Rev. Lett. **77**, 2810 (1996).
- [70] A. Kirilyuk, Th. Rasing, R. Mégy, and P. Beauvillain, Phys. Rev. Lett. **77**, 4608 (1996).
- [71] W. Weber, A. Bischof, R. Allenspach, C. Würsch, C.H. Back, and D. Pescia, Phys. Rev. Lett. **76**, 3424 (1996).
- [72] C.H. Back, W. Weber, C. Würsch, A. Bischof, D. Pescia, and R. Allenspach, J. Appl. Phys. **81**, 5054 (1997).
- [73] M.R. Halse, Philos. Trans. R. Soc. London A **265**, 507 (1969).
- [74] M.T. Johnson, S.T. Purcell, N.W.E. McGee, R. Coehoorn, J. aan de Stegge, and W. Hoving, Phys. Rev. Lett. **68**, 2688 (1992).
- [75] W. Weber, R. Allenspach, and A. Bischof, Europhys. Lett. **31**, 491 (1995).
- [76] J. Unguris, R.J. Celotta, and D.T. Pierce, J. Magn. Magn. Mater. **127**, 205 (1993).
- [77] A. Fuss, S. Demokritov, P. Grünberg, and W. Zinn, J. Magn. Magn. Mater. **103**, L221 (1992).
- [78] J. Unguris, R.J. Celotta, and D.T. Pierce, J. Appl. Phys. **75**, 6437 (1994).
- [79] J. Unguris, R.J. Celotta, and D.T. Pierce, Phys. Rev. Lett. **79**, 2734 (1998).
- [80] S.S.P. Parkin, R. Bhadra, and K.P. Roche, Phys. Rev. Lett. **66**, 2152 (1991).
- [81] D.H. Mosca, F. Pétroff, A. Fert, P.A. Schroeder, W.P. Pratt, Jr., R. Laloe, and S. Lequien, J. Magn. Magn. Mater. **94**, L1 (1991).
- [82] F. Pétroff, A. Barthémy, D.H. Mosca, D.K. Lottis, A. Fert, P.A. Schroeder, W.P. Pratt, Jr., R. Laloe, and S. Lequien, Phys. Rev. B **44**, 5355 (1991).
- [83] J.J. de Miguel, A. Cebollada, J.M. Gallego, R. Miranda, C.M. Schneider, P. Schuster, and J. Kirschner, J. Magn. Magn. Mater. **93**, 1 (1991).
- [84] S.N. Okuno and K. Inomata, Phys. Rev. Lett. **70**, 1771 (1993).

- [85] S.S.P. Parkin, C. Chappert, and F. Herman, *Europhys. Lett.* **24**, 71 (1993).
- [86] J.-F. Bobo, L. Hennet, and M. Piécuch, *Europhys. Lett.* **24**, 139 (1993).
- [87] P. Bruno, Los Alamos Preprint Server, <http://xxx.lanl.gov/cond-mat/9808091>
- [88] P. Bruno, *Europhys. Lett.* **23**, 615 (1993).
- [89] P.J.H. Bloemen, M.T. Johnson, M.T.H. van de Vorst, R. Coehoorn, J.J. de Vries, R. Jungblut, J. aan de Stegge, A. Reiders, and W.J.M. de Jonge, *Phys. Rev. Lett.* **72**, 764 (1994).
- [90] S.N. Okuno and K. Inomata, *Phys. Rev. Lett.* **72**, 1553 (1994).
- [91] J.J. de Vries, A.A.P. Schudelaro, R. Jungblut, P.J.H. Bloemen, A. Reinders, J. Kohlhepp, R. Coehoorn, and de W.J.M. Jonge, *Phys. Rev. Lett.* **75**, 1306 (1995).
- [92] S.N. Okuno and K. Inomata, *J. Phys. Soc. Japan* **64**, 3631 (1995).
- [93] A. Bounouh, P. Beauvillain, P. Bruno, C. Chappert, R. Mégy, and P. Veillet, *Europhys. Lett.* **33**, 315 (1996).
- [94] P. Bruno, *J. Magn. Magn. Mater.* **164**, 27 (1996).
- [95] J. Kudrnovský, V. Drchal, P. Bruno, I. Turek, and P. Weinberger, *Phys. Rev. B.* **56**, 8919 (1997).
- [96] P. Hohenberg and W. Kohn, *Phys. Rev.* **136**, B864 (1964).
- [97] W. Kohn and L.J. Sham, *Phys. Rev.* **140**, A1133 (1965).
- [98] U. von Barth und L. Hedin, *J. Phys. C: Solid State Phys.* **5**, 1629 (1972).
- [99] P.H. Dederichs, S. Blügel, R. Zeller, and H. Akai, *Phys. Rev. Lett.* **53**, 2512 (1984).
- [100] A.R. Mackintosh and O.K. Andersen, in *Electrons at the Fermi Surface*, edited by M. Springford (Cambridge University Press, Cambridge, England, 1980), p. 149.
- [101] M. Weinert, R.E. Watson, and J.W. Davenport, *Phys. Rev. B* **32**, 2115 (1985).
- [102] J. Harris, *Phys. Rev. B* **31**, 1770 (1985).
- [103] W.M.C. Foulkes and R. Haydock, *Phys. Rev. B* **39**, 12520 (1989).
- [104] A.J. Read and R.J. Needs, *J. Phys.: Condens Matter* **1**, 7565 (1989).
- [105] M.W. Finnis, *J. Phys.: Condens. Matter* **2** 331, (1990).
- [106] I.J. Robertson and B. Farid, *Phys. Rev. Lett.* **66**, 3265 (1991).
- [107] J. Kudrnovský, V. Drchal, and I. Turek, private communication.

- [108] P. Bruno, J. Kudrnovský, V. Drchal, and I. Turek, Phys. Rev. Lett. **76**, 4253 (1996).
- [109] F. Ducastelle, J. Phys. C: Solid State Phys. **8**, 3297 (1975).
- [110] J. Kudrnovský, V. Drchal, P. Bruno, I. Turek, and P. Weinberger, Phys. Rev. B **54**, 3738 (1996).